Development of a Non-stationary Standardized Precipitation Evapotranspiration Index (NSPEI) for Drought Monitoring in a Changing Climate

Javad Bazrafshan (jbazr@ut.ac.ir)
University of Tehran https://orcid.org/0000-0002-6721-8990
Majid Cheraghalizadeh
University of Tehran
Kokab Shahgholian
University of Tehran

Research Article

Keywords: Drought, Non-stationary, SPEI, NSPEI, GAMLSS, Iran

Posted Date: June 9th, 2021

DOI: https://doi.org/10.21203/rs.3.rs-573309/v1

Development of a Non-stationary Standardized Precipitation Evapotranspiration Index (NSPEI) for Drought Monitoring in a Changing Climate

Javad Bazrafshan[1], Majid Cheraghalizadeh[2], Kokab Shahgholian[3]

[1]Corresponding Author, Associate Professor, Department of Irrigation and Reclamation Engineering, University of Tehran, Karaj, Iran. Email: jbazr@ut.ac.ir

[2]PhD Student, Department of Irrigation and Reclamation Engineering, University of Tehran, Karaj, Iran. Email: majid_ab86@yahoo.com

[3]PhD Student, Department of Irrigation and Reclamation Engineering, University of Tehran, Karaj, Iran. Email: nadiashahgholian@gmail.com

Abstract

In a changing climate, drought indices as well as drought definitions need to be revisited, because some statistical properties, such as long-term mean, of climate series may change over time. The study aims to develop a Non-stationary Standardized Precipitation Evapotranspiration Index (NSPEI) for reliable and robust quantification of drought characteristics in a changing environment. The proposed indicator is based on a non-stationary log-logistic probability distribution, assuming the location parameter of the distribution is a multivariable function of time and climate indices, as covariates. The optimal non-stationary model was obtained using a forward selection method in the framework of Generalized Additive Models in Location, Scale and Shape (GAMLSS) algorithm. The Non-stationary and Stationary forms of SPEI (i.e. NSPEI and SSPEI) were calculated using the monthly precipitation and temperature data of 32 weather stations in Iran for the common period of 1964-2014. The results showed that almost at all the stations studied, the non-stationary log-logistic distributions outperformed the stationary one. Both drought indicators SSPEI and NSPEI significantly differed in terms of spatial and temporal variations of drought characteristics. While SSPEI identified the long-term and continuous drought/wet events,

NSPEI revealed the short-term and frequent drought/wet periods at almost all the stations of interest. Finally, it was revealed that NSPEI, compared to SSPEI, was a more reliable and robust indicator of drought duration and drought termination in vegetation cover during the severest drought period (the 2008 drought), and therefore, was suggested as a suitable drought index to quantify drought impact on vegetation cover in Iran.

Keywords: Drought; Non-stationary; SPEI; NSPEI; GAMLSS; Iran.

1. Introduction

Drought, as a recurrent and normal feature of climate, affects economy, society, and environment across the globe (Wilhite 2000). Historical evidence shows that Iran has suffered from the long-term and devastating droughts during few centuries ago. For instance, the intensive famines during 1870-1872 and 1917-1919 which occurred due to drought occurrences, endangered water and food security throughout the country, and destroyed half of the population (De Planhol 2012). Bazrafshan et al. (2017) specified that during 1894-2010, Iran (with average annual precipitation of 254 mm) had experienced 23 drought events, ranging from 1 to 10 years. The 2008-2010 and 1998-2002 droughts, with total precipitation deficits of 176.1 and 180.4 mm, respectively, were identified as the most severe and extensive drought events. As reported by OFDA/CRED (2015), drought was ranked first among all natural hazards in Iran based on the number of people affected during 1900-2015.

Drought is conventionally defined as a temporary period of moisture deficit relative to the long-term average at a given location (Mishra and Singh 2010, Paulo and Pereira 2006, Van Loon 2015). This simple definition, however, cannot be used in the regional studies of drought. To this end, drought indices are used. Using standardization of moisture deficiencies, drought indices enable us to compare different locations based on their drought characteristics (such as severity and duration) (Şen 2015). These indices have been used to monitor meteorological, agricultural, and hydrological droughts (Wilhite and Glantz 1985).

The origin of all droughts starts from lack of precipitation (meteorological drought). It gradually spreads to the other sectors in the form of deficiency in soil moisture (agricultural drought) and reduction of surface water and groundwater resources (hydrological drought) (Bhardwaj et al. 2020, Huang et al. 2017, Van Lanen 2006). Therefore, the accurate monitoring of meteorological drought would be very important in predicting agricultural and hydrological droughts. In this research, meteorological drought is considered.

Precipitation and evapotranspiration are the two main variables of meteorological drought indices (Beguería et al. 2014, Tirivarombo et al. 2018, Vicente-Serrano et al. 2010). In the energy-limited areas such as humid and rainy areas of northern Iran, precipitation alone is sufficient to monitor meteorological drought. In the water-limited areas such as the hyper arid and semi-arid regions of Iran, in addition to precipitation, atmospheric evaporative demand (AED) also plays a crucial role and need to be taken into account for effective drought monitoring and management (Bazrafshan 2017).

During the last two decades, the Standardized Precipitation Index (SPI), developed by McKee et al. (1993), have been widely used for assessing the temporal and spatial variations of meteorological droughts across the globe. The first feature of SPI is that it is dimensionless, which allows the index to be comparable in different geographical locations. The other feature of SPI is its ability to be calculated on multiple timescales (short-term, medium-term, and long-term) that provide a projection of the drought occurrence in soil, surface water and groundwater resources (Mishra and Singh, 2011). The SPI substantially fits the appropriate probability distribution (e.g. Gamma) to a series of cumulative precipitation at a given timescale, and then, transforming the probability of any cumulative precipitation value to the standard normal variate (called SPI) (Guenang and Kamga 2014, WMO 2012). The mathematical algorithm governing this index became so popular that several drought indices (both univariate and multivariate) were developed based on the same mathematical

algorithm (Bateni et al. 2018, Bazrafshan et al. 2014, Vicente-Serrano et al. 2010). One of the drought indices that follows the mathematical algorithm of SPI is the Standardized Precipitation Evapotranspiration index (SPEI) (Vicente-Serrano et al. 2010). Instead of the precipitation deficiency with respect to the long-term average, SPEI is calculated based on the precipitation shortage with respect to AED at multiple timescales. Also, instead of a stationary Gamma distribution, it uses a stationary three-parameter log-logistic distribution (Beguería et al. 2014, Hernandez and Uddameri 2014, Vicente-Serrano et al. 2010). SPEI has all the benefits of SPI. A feature that makes SPEI superior to SPI is that it can incorporate the effect of global warming into the severity of drought. This effect appeared in the initial version of SPEI, in which monthly mean temperature was used to calculate AED from the Thornthwaite method (Thornthwaite 1948). The issue of selecting the appropriate method for calculating AED can be crucial in the SPEI computation, because the method of calculating AED may significantly affect the SPEI results. For example, Zarei and Mahmoudi (2020) examined the effect of different methods of calculating AED on the SPEI calculations at a number of meteorological stations in Iran. Using some statistical tests and metrics, they indicated that there were no significant differences between the SPEIs calculated by the method Thornthwaite (1948) and those calculated by the FAO Penman-Monteith reference method (Allen et al. 1998). Mavromatis (2007) also showed that the use of simple and complex methods to calculate AED in a drought index such as Palmer Drought Severity Drought Index (PDSI) produced similar results.

Climate change, in the most optimistic case, will change the average of climatic elements such as precipitation and air temperature (IPCC 2014), and this change in the average would not be consistent with the existing definitions of droughts. Therefore, definition of drought in a changing climate needs to be revisited. The main effects of future climate change are the regional increase/decrease of precipitation and the global increase in

air temperature (IPCC 2014). Under stationary climatic conditions and assuming low variability of other climatic factors such as air temperature, the traditional SPI is capable of representing the effect of precipitation variations on drought (Russo et al. 2013). Under non-stationarity of precipitation data, the development of a Non-stationary SPI (NSPI) for drought assessment has been proposed (Li et al. 2015, Rashid and Beecham 2019, Wang et al. 2015). Although the NSPI considers the precipitation changes in a changing climate, it, like the SPI, is unable to demonstrate the effect of global warming on drought characteristics (Asadi Zarch et al. 2015). In such condition, as stated earlier, the SPEI may be a suitable option. However, SPEI calculations are also reliable under assumption of climate stationarity.

Incorporating the environmental changes in the context of drought indices is an important issue which is not regarded in the traditional drought indices (Li et al. 2015). So far, efforts have been made to develop drought indices under climate non-stationarity. According to literature, the first study in this context was carried out by Russo et al. (2013). They believed that the effect of climate change signals on climate variables for the periods longer than 30 years is significant, and therefore, the results of drought indices such as SPI would not be reliable due to the changes in the statistical parameters (especially, location parameter) of Gamma distribution for those long periods. To overcome this issue, they developed a non-stationary Gamma distribution in the SPI structure and called the new index as the Standardized non-stationary Precipitation Index (SnsPI). Wang et al. (2015) proposed a time-dependent Standardized Precipitation Index (SPIt) in the Luanhe River Basin, China. Non-stationarity in SPIt was modeled by fitting a Gamma distribution with a time-dependent location parameter to the summer precipitation data. Non-stationary models were introduced as polynomial regression functions with the degrees less than or equal to 3 of time within the Generalized Additive Models in Location, Scale and Shape (GAMLSS) framework. The optimal non-stationary model was selected by minimizing the Akaike Information Criterion

(AIC) (Akaike 1974) and the Schwarz Bayesian Criterion (SBC) (Schwarz 1978). The results showed that in most situations, the non-stationary Gamma distribution has a better fit to the precipitation series compared to its stationary form; therefore, SPIt was introduced as a more reliable and robust drought index than SPI in the study river basin. Bazrafshan and Hejabi (2018) developed a Non-stationary Reconnaissance Drought Index (NRDI) for drought monitoring in a changing climate in Iran. They considered the location parameter of the log-normal probability distribution as a polynomial regression function of time. Both stationary and non-stationary forms of log-normal distribution were fitted to the series of the precipitation to evapotranspiration ratio at different timescales. Results showed that, in most stations, the non-stationary log-normal distribution was able to simulate the monotonic downward trend identified by the Mann-Kendall test, and outperformed the stationary one.

One of the important limitations of time-dependent drought indices such as SnsPI, SPIt, and NRDI is that the assumption of the linear relationship of distribution parameters with time is not always true in the future behavior of climate data, because this linear relationship may be part of a larger cycle which are not manifest in current data (Li et al. 2015). Furthermore, the time-dependent non-stationary models cannot accurately represent the variability in distribution parameters (Serinaldi and Kilsby 2015). To resolve this issue, the climate signals such as ENSO and NAO were proposed as the explanatory variables (or covariates) in some studies, as follow. Li et al. (2015) developed a Non-stationary Standardized Precipitation Index (NSPI) in the Luanhe River Basin, China. They used a number of large-scale climate indices, as covariates, to estimate the location parameter of Gamma distribution on the basis of three groups of models (i.e. stationary, time-dependent non-stationary, and the climate index-dependent non-stationary). They concluded that the climate index-dependent non-stationary models outperformed the other two groups; hence, the time-dependent models proposed in the study of Wang et al. (2015) were not suitable for

drought assessment in the same basin. Also, due to the fact that the non-stationary models use the lagged values of climate indices, the variability of the distribution parameters over time is maintained in the NSPI calculations. Additionally, the NSPI was able to simulate well the historical droughts of the basin as well as their spatiotemporal characteristics. Wang et al. (2020) presented a Non-stationary Standardized Streamflow Index (NSSI) in the Luanhe River Basin of China. The NSSI considers the non-stationarities caused by both the climatic and anthropogenic effects on the river flow. The climatic effects were incorporated into the framework of non-stationary models using the climate indices (i.e. teleconnections) and the anthropogenic effects using the Soil and Water Assessment Tools (SWAT) model. Results showed that NSSI describes the temporal and spatial variability of the river flow better than the Standardized Streamflow Index (SSI). Kang and Jiang (2019) offered a standardized streamflow index for monitoring hydrological drought under the environmental change conditions of China's Yangtze River. The statistical tests did not confirm the stationary assumption of the streamflow data. Therefore, the two covariates, time and modified reservoir index, were applied to model the non-stationarity in the streamflow data. They concluded that the modified reservoir index incorporated in the non-stationary model reported more severe droughts than the stationary one. However, the time-dependent non-stationary model underestimated the risk of drought events. Rashid and Beecham (2019) developed a Non-stationary Standardized Precipitation Index (NSPI) within the GAMLSS algorithm for drought monitoring in South Australia. They used climate signals as covariates to model the non-stationarity in precipitation data. The results showed the superiority of the non-stationary models to the stationary model in representing drought characteristics. They concluded that the recurrence period of the drought events of larger than any amount of drought severity and duration estimated by NSPI was significantly different from those of the Stationary Standardized Precipitation Index (SSPI).

As mentioned earlier, in a changing environment where either both precipitation and AED variables or one of them are non-stationary, the drought assessment and the statistical analyses based on the stationary assumption of data would not be reliable. Therefore, in the continuation and progression of the previous studies, there will be a need to develop the non-stationary form of SPEI for more robust and reliable monitoring of meteorological drought in a changing climate. The purpose of this study is to propose a Non-stationary Standardized Evapotranspiration Precipitation Index (NSPEI) under changing climate conditions in Iran. Non-stationary modeling of climate variables is carried out using the covariates, namely, time and the teleconnections, such as ENSO and NAO, affecting the climate of Iran. Both stationary and non-stationary indices are compared in terms of several temporal and spatial drought characteristics. Finally, the temporal variations of vegetation cover and both stationary and non-stationary drought indices were evaluated during the severest drought period (the 2008 drought) in Iran, in order to introduce a suitable drought index to monitor drought impact on vegetation cover.

2. Materials and Methods

2.1. Study Area: Geographical Characteristics, Climate, and Teleconnections

Geographically, Iran is located in West Asia in the range of 63°– 44° East longitude and 29°–35° North latitude. Most of Iran's climate is arid (64%) and semi-arid (20%), due to its location in the subtropical high-pressure subsidence zone. In addition, about 16% of its area is Mediterranean to very humid (Khalili 1997). The main controllers of Iran's climate are: latitude, altitude, and distance from the seas and oceans. The latitudinal expanse of Iran, in fact, directly affects the solar radiation and temperature regimes of its different regions. The Alborz Mountains in the north and the Zagros Mountains in the west of the country act as walls that prevent moisture from reaching the central parts of the country, and as a result, create two very dry and hot deserts, Kavir and Lut, in those regions. Iran's climate is also

influenced by the near (Caspian Sea, the Persian Gulf and Oman Sea) and distant (Black Sea, Mediterranean Sea, Indian Ocean, Atlantic Ocean, and the Red Sea) water bodies (Khalili and Rahimi 2018). The main sources of precipitation in Iran are the low pressures (mainly Mediterranean) that influence the spatial and temporal distribution of precipitation directly during seven months of the year from mid-October to mid-March (Khalili and Rahimi 2014). Siberian's high pressure also plays an important role in the precipitation occurrence on the southern shores of the Caspian Sea in November and December. Precipitation amount decreases from the west to the east and from the north to the south of the country. The long-term average annual precipitation in Iran is 254 mm, which varies between 13 mm and 2003 mm across the country. The long-term average temperature in the country varies between 1.6℃ (at the elevation of 3000m) to 28℃ (on the southern coast) (Khalili 1997, Khalili and Rahimi 2018). Generally, climate change is expected to make the country warmer and drier in the future (Bazrafshan 2017, Rahimi et al. 2013, Vaghefi et al. 2019).

There are a large number of studies that connect large-scale atmospheric–oceanic phenomena (i.e. teleconnections) to the occurrence of droughts/floods in different parts of the country in different seasons of the year. Research in this context suggests that four teleconnections, namely El Niño–Southern Oscillation (ENSO), North Atlantic Oscillation (NAO), Arctic Oscillation (AO), and North Caspian Sea Pattern (NCP), have major effects on climate variability in Iran, as discussed below:

i. ENSO: In the majority of the country, autumn precipitation increases during the positive phase of ENSO (i.e. El Niño), and winter and summer precipitation decreases. In addition, a severe La Niña (the negative phase of ENSO) intensify the probability of dry conditions in autumn and the probability of wet condition in winter and summer (Golian et al. 2015, Nazemosadat and Cordery 2000, Nazemosadat and Ghasemi 2004).

ii. NAO: The strong NAO is associated with high precipitation and low temperature in winter in most region of Iran (Moradi 2004).

iii. AO: Air temperature in winter is negatively associated with AO in most parts of Iran. This means that the positive (negative) air temperature anomalies are correlated with the negative (positive) AO phases (Ghasemi and Khalili 2006).

iv. NCP: NCP's positive (negative) phase accords with the increase (decrease) in Iran's winter precipitation. The colder (warmer) than normal winter temperature in Iran is consistent with the positive (negative) phase of NCP (Ghasemi and Khalili 2008).

2.2. Data

In this study, three different datasets were used:

i. Local-scale climate data, measuring at weather stations, were employed to calculate drought indices. The monthly precipitation and air temperature data recorded at 32 weather stations (Fig. 1) in Iran cover a common period from 1964 to 2014. The data were procured from IR of Iran Meteorological Organization (IRIMO). Preliminary assessments of the data showed that 18 out of 32 stations had no missing values during the record period. Missing data of a given station (i.e. the base station) were filled using a regression equation between the base station and a neighboring station of complete data that was strongly correlated with the base station (Sattari et al. 2017).

ii. Large-scale climate indices (teleconnections), occurring at far distances over oceans, were used as covariates within the non-stationary models. The monthly data of ENSO, NAO, and AO were downloaded from the webpage of NOAA (https://www.ncdc.noaa.gov/teleconnections/) and those of NCP from the webpage of CRU (https://crudata.uea.ac.uk/cru/data/ncp/ncp.dat).

iii. Normalized Difference Vegetation Index (NDVI) data, being the product of NOAA Global Inventory Monitoring and Modeling System (GIMMS), version 3g.v1, were

used to monitor the drought occurrence in vegetation cover. The temporal resolution of the product is twice a month (each 15 days) with a 0.083° by 0.083° spatial grid resolution. The data covered the period of July 1981 to December 2015 (Pinzon and Tucker 2014), and are available from the webpage (https://ecocast.arc.nasa.gov/data/pub/gimms/3g.v1).

2.3. Methods

2.3.1. Standardized Precipitation Evapotranspiration Index (SPEI)

The Standardized Precipitation Evapotranspiration Index (SPEI), as a climatic drought index, was proposed by Vicente-Serrano et al. (2010). Calculation of SPEI includes several steps, as follow:

i. Calculation of a simple climatic water balance according to the following equation:

$$D_i = P_i - AED_i \qquad (1)$$

where D_i is the difference between precipitation (P_i) and atmospheric evaporative demand (AED_i) in the month number i in the time series ($i = 1$ indicates the first data of time series and $i = n$ is the last data of time series). As justified in the Introduction section, the method of Thornthwaite (1948) was used to calculate AED in this study. In addition, the method requires only monthly mean air temperature data, which is easily accessible from many weather stations across the study area.

ii. Selection of timescale: In this research, SPEI was calculated at 12-month timescale due to the management of Iran's water resources on the water-year scale (i.e. from October of the current year to September of next year) (Raziei et al. 2008). Likewise, the 12-month timescale is the most prevailing precipitation cycle across the world (Byun and Wilhite 1999).

iii. Moving aggregation of consecutive D-values at a given timescale:

$$x_{t,k} = \sum_{i=t-k+1}^{t} D_i \qquad for\ t \geq k \qquad (2)$$

where $x_{t,k}$ is the cumulative D-values of the k-month timescale (here $k = 12$) at the time t ($t = 1, 2, \ldots, n$) and is called the x-series, hereafter.

iv. Fitting a suitable probability distribution function to the x-series. According to the studies of Vicente-Serrano et al. (2010), the three-parameter log-logistic distribution has the flexibility to fit appropriately the x-series worldwide, with assuming the temporal stationarity of the series. The mathematical form of the probability density function of the above-mentioned distribution is expressed as below:

$$f(x) = \frac{\beta}{\alpha}\left(\frac{x-\gamma}{\alpha}\right)^{\beta-1}\left[1 + \left(\frac{x-\gamma}{\alpha}\right)^{\beta}\right]^{-2} \qquad (3)$$

where α, β and γ are the parameters of scale, shape and location of the distribution, respectively, and x is the cumulative series of D-values at a given timescale. The parameters of this function are obtained using the L-moment method (Hosking, 1990) from the following equations:

$$\beta = \frac{2w_1 - w_0}{6w_1 - w_0 - 6w_2} \qquad (4)$$

$$\alpha = \frac{(w_0 - 2w_1)\beta}{\Gamma(1+\frac{1}{\beta})\Gamma(1-\frac{1}{\beta})} \qquad (5)$$

$$\gamma = w_0 - \alpha\Gamma(1 + \frac{1}{\beta})\Gamma(1 - \frac{1}{\beta}) \qquad (6)$$

where $\Gamma(.)$ is the Gamma function and w_0, w_1 and w_2 are the probability weighting moments calculating from the following equation:

$$w_s = \frac{1}{n}\sum_{m=1}^{n}(1 - F_m)^s D_m \qquad (7)$$

where F is the empirical distribution function, n is the total number of data, m is the rank of data in the ascending order, and s is the moment order, and here it is considered zero, 1, and 2 to calculate the terms w_0, w_1 and w_2, respectively, in Eq. (4-6). The value of F is calculated from the empirical function (Hosking 1990), as below:

$$F_m = \frac{m - 0.35}{n} \qquad (8)$$

The log-logistic cumulative distribution function of x is defined by the expression:

$$F(x) = \left[1 + (\frac{\alpha}{x-\gamma})^{\beta}\right]^{-1} \quad (9)$$

v. Calculation of SPEI: The cumulative probability of any value of x (i.e. $F(x)$) is transformed to the standard normal variate (with mean zero and variance one), so-called SPEI. Using the approximation of Abramowitz and Stegun (1965), the cumulative probability is transformed to the standard normal variate (i.e. the SPEI equation), as follows:

$$SPEI = W - \frac{C_0 + C_1 W + C_2 W^2}{1 + d_1 W + d_2 W^2 + d_3 W^3} \quad (10)$$

in which,

$$W = \sqrt{-2\, ln(P)} \quad for \quad P \leq 0.5 \quad (11)$$

and $P = 1 - F(x)$. If $P > 0.5$, $1 - P$ is substituted for P in Eq. (11). The constants in the SPEI equation are:

$$C_0 = 2.515517, \quad C_1 = 0.802853, \quad C_2 = 0.010328$$

$$d_1 = 1.432788, \quad d_2 = 0.189269, \quad d_3 = 0.001308$$

Since the traditional SPEI is calculated under stationary condition; henceforth, we call it the Stationary SPEI (SSPEI). The SSPEI classification is described in Table 1. The negative values of SSPEI demonstrate the dry periods (droughts) and the positive values of SSPEI imply the wet periods.

2.3.2. Non-stationary SPEI (NSPEI)

The methodology of Non-stationary Standardized Precipitation Evapotranspiration Index (NSPEI) is presented in Fig. 2. While the SSPEI assumes all parameters of the log-logistic distribution fitted to the x-series (the cumulative D-values) are constant (stationary), the NSPEI fits an optimal non-stationary model to the series. The non-stationary statistical model assumes that one or more parameters of the log-logistic parameter vary as a function of some

external covariates. The external covariates selected in this study are the time variable and the climate indices influencing the precipitation and air temperature in Iran, namely ENSO, NAO, AO, and NCP (Alizadeh-Choobari et al. 2018, Dezfuli et al. 2010, Ghasemi and Khalili 2006, 2008). Many researchers believe that climate change, in most probable case, changes the average of climate variables in the regional or global scale (Cheng and AghaKouchak 2014, Kwon and Lall 2016, Li et al. 2015, Russo et al. 2013, Wang et al. 2015). The non-stationary models used in the study assume that the location parameter of log-logistic distribution is a multivariable function of the covariates as below:

$$\gamma(t) = a_0 + a_1 t + b_1 C_1(t-l) + \cdots + b_m C_m(t-l) \tag{12}$$

where $\gamma(t)$ is the location parameter at time t, a_0 is the intercept, $b_1, \ldots, b_m$ are the regression coefficients, $C_1(t-l), \ldots, C_m(t-l)$ are the climate indices at time $t-l$ in which l is the lag-times $0, 1, \ldots, 12$ months. The other parameters of the log-logistic distribution are assumed to be constant. The optimal combination of the variables in Eq. (12) for each month of the year at 12-month timescale is selected using the forward selection method in the framework of Generalized Additive Models in Location, Scale and Shape (GAMLSS) algorithm (Rigby and Stasinopoulos 2005). In this study, GAMLSS is applied to model a non-stationary log-logistic distribution using a (semi) parametric relationship between the location parameter $\gamma(t)$ and each combination of the covariates through the monotonic link function ($g(.)$), as below:

$$g(\gamma) = X\alpha + \sum_{j=1}^{J} Z_j(\beta_j) \tag{13}$$

where α is a parameter vector of size J, X is a fixed, known design vector of size J, β_j is a vector of random effects parameters having normal distribution, Z_j is a non-parametric additive function of β_j. All parameters are estimated using the maximum (penalized) likelihood estimator (Stasinopoulos et al. 2008).

Eq. (13) is evaluated for different combinations from 1 to 5 variables corresponding to the five covariates used in this study. The best non-stationary model is one with the least AIC value (AICmin). If the differences between the AIC of the best model and the AICs of some of the remaining ones are less than 2, the optimal model is that with a number of covariates lower than the best one (Burnham and Anderson 2002). It is worth noting that, with the support of the GAMLSS package incorporated into the R software, the computation processes for evaluation of the non-stationary models were accomplished (Stasinopoulos et al. 2008).

In order to calculate NSPEI, the cumulative probability corresponding to any values of the x-series is estimated from the non-stationary log-logistic distribution, and then, is transformed inversely to the standard normal variate (here called NSPEI). Classification of the NSPEI is like the SSPEI, as shown in Table 1. The NSPEI values less than zero imply the dry conditions (droughts) and those equal to or more than zero indicate the wet conditions.

2.3.3 Vegetation Condition Index

The Vegetation Condition Index (VCI), which was firstly proposed by Kogan (1995), is a NDVI-based remote sensing drought index which is computed using the following formula:

$$VCI = \frac{NDVI - NDVI_{min}}{NDVI_{max} - NDVI_{min}} \times 100 \qquad (14)$$

where $NDVI$ is the smoothed monthly NDVI, and $NDVI_{min}$ and $NDVI_{max}$ are the multi-year minimum and maximum NDVI values, respectively, in each grid cell in each month of the year. VCI ranges from 0% to 100%, showing extremely unfavorable to optimal conditions of vegetation. Unlike the NDVI which represents the compound effect of weather and ecology in drought monitoring, the VCI is able to separate the ecology component from the NDVI data and to quantify only the effect of meteorological droughts on vegetation (Rahimzadeh Bajgiran et al. 2008, Shamsipour et al. 2008).

In this study, the VCI was calculated from the NDVI averaged over a 3×3 window, including the nine pixels around the position of each weather station (Rahimzadeh Bajgiran et al. 2008). Then, a 12-month moving average method, like the SSPEI and NSPEI, was applied to the VCI series. A drought event in vegetation happens when the VCI be less than 40% (Ghaleb et al. 2015). Temporal variations in vegetation over the study area were assessed in association with SSPEI and NSPEI to determine the necessity of incorporating the non-stationary framework into the SPEI calculations.

2.3.4 The Orientation and Magnitude of Trend

A nonparametric Mann-Kendall (MK) statistical test (Kendall 1970, Mann 1945) is employed to evaluate the trend orientation in P, AED, and *x*-series at all stations of interest. Considering the serially independent data $u_i, i = 1, 2, \ldots, n$, in which n is the length of data, the MK test statistic Z is defined as:

$$Z = \begin{cases} \frac{S-1}{\sqrt{Var(S)}} & , \ S > 0 \\ 0, & S = 0 \\ \frac{S+1}{\sqrt{Var(S)}} & , \ S < 0 \end{cases} \qquad (15)$$

where S is sum of the sign function values according to the following formula:

$$S = \sum_{i=1}^{n-1} \sum_{j=i+1}^{n} sgn(u_i - u_j) \qquad (16)$$

and $Var(S)$ is the variance of S which is defined as:

$$Var(S) = \frac{1}{18}[n(n-1)(2n+5) - \sum_{p-1}^{g} t_p(t_p - 1)(2t_p + 5)] \qquad (17)$$

where g is the number of tied groups and t_p is the number of observations in the pth group. The no trend hypothesis is rejected if $|Z| > Z_{1-\alpha/2}$ in which $Z_{1-\alpha/2}$ follows the standard normal variate at the significance level of α. A positive (negative) significant value of Z indicates an upward (downward) monotonic trend. Note that the lag-1 autocorrelations in data series were removed prior the data to be further analyzed for trend detection, according to the approaches presented in Hamed and Ramachandra Rao (1998) and Yue et al. (2002).

In addition to the orientation of trend, the magnitude of the trend in data series is estimated using the Sen's slope estimator (Sen 1968). The median of slopes (b) for any two time points of data is determined by the following equation:

$$b = Median\left(\frac{u_j - u_i}{j - i}\right) \quad , \quad 1 \leq i < j \leq n \qquad (18)$$

3. Results and Discussions

3.1. Trend Analysis

Table 3 shows the orientation and magnitude of trends in precipitation (P), atmospheric evaporative demand (AED), and P-AED (i.e. D). As shown in this table, using the MK test, 59.4% and 6.3% of the stations detected the significant negative and positive trends, respectively, in precipitation data at the 5% significance level. The MK test revealed more significant positive trends (50.0% of stations) than negative trends (40.6% of stations) in AED. While some stations (e.g. Ahvaz, Birjand, and Gorgan) experienced a downward trend in both P and AED, some other stations (e.g. Esfahan and Tehran-Mehrabad) indicated an upward trend in both of the above variables. In several stations, the trend orientation in P was opposite to that in AED (for example, at Bandar Anzali, while P showed a downward trend, AED indicated an upward trend). The magnitude of the trend across the studied stations ranged from -2.78 (Gorgan) to 1.07 (Esfahan) mm/decade for P, and from -3.32 (Shahrekord) to 9.15 (Abadan) mm/decade for AED.

With respect to P and AED as the two components of D, the magnitude of trends for both variables determines the direction of the temporal trend in D. According to Table 3, the trend magnitude of AED in most stations are larger than those of P; thus, the direction and slope of the trend in D is predicted to be more determined by AED than by P. This is supported by the strong correlation between the trend magnitudes in D vs. the trend magnitudes in AED compared to the trend magnitudes in D vs. the trend magnitudes in P, as

seen in Fig. 3. It can therefore be said with great confidence that a downward (upward) trend in AED leads to an upward (downward) trend in D. Referring to Table 3, it can be found that the MK test reported significant positive and negative trends in 18.7% and 59.4% of the stations, respectively. These findings indicate that the water deficit has intensified with time in more than half of the stations of interest. In addition, at most stations, the D series are non-stationary, and thus the development of a drought index that is consistent with changing climate is necessary.

3.2. Teleconnection between the x-Series and Climate Indices

Fig. 3 displays the boxplot of the Spearman correlation coefficients between the 12-month aggregated D-values (i.e. the x-series) and each of the four selected climate indices (ENSO, AO, NCP, and NAO) used in this study for the 0- to 12-month lag-times. As can be seen in the figure, while the x-series has negative correlations with ENSO, its correlations with the other three climate indices are mostly positive. The x-series have significant correlations with ENSO in more than half of the stations for the 0- to 1-month lag-times and, with the lag-times increasing to 12 months, the correlations become non-significant. In a number of stations, correlations of x-series with AO, NCP, and NAO are significant for the lag-times longer than five months, shorter than eight months, and 0-1 and longer than seven months, respectively. The results showed the relative significance of ENSO, compared to the other three indices, in describing the behavior of the x-series at the stations of interest.

3.3. Selection of the Optimal Non-stationary Models

Table 4 shows the step-by-step forward selection of the covariates (namely t, ENSO, AO, NCP, and NAO) for estimation of the location parameter of log-logistic distribution at the stations of interest for the 12-month sub-period of October-September. The selection process for suitable variables was carried out in five consecutive steps, according to Eq. (12). The variables were chosen for their significance in estimating the location parameter; the most

important variable in the first position and the other variables occupy the second to fifth position. In this selection method, five non-stationary models with a combination of 1 to 5 variables were constructed to estimate the location parameter at the studied stations. For example, as shown in Table 4, at Abadan station, according to the AIC values in the steps (1)-(5), the bivariate model with covariates t and $NCP(t-5)$ has the lowest AIC value and is considered as the best non-stationary model to estimate the location parameter. However, the univariate model in step (1), which has only the t-covariate, has been selected as the optimal model because the difference between the AIC of the optimal model and that of the best model is not significant and the number of variables used in the optimal model is less than the best model. Also, the selected optimal model has AIC=720 that is less than the AIC of the stationary model (743.3). The non-stationary optimal models outperformed the stationary model at almost all stations except Kerman station. This result is valid for all other sub-periods, in addition to the sub-period of October-September.

Table 5 shows the mathematical formulae of the optimal non-stationary models to estimate the location parameter of log-logistic distribution at the studied stations for the 12-month sub-period of October-September. As mentioned above, a time-dependent model is sufficient to model the non-stationarity of the location parameter at Abadan station (#1). If time is a strong covariate in the model, it should also be verified by the non-parametric Mann-Kendall (MK) test. As can be seen in Table 5, the MK statistic at this station is significant at the 99% confidence level. The negative slope of t in the optimal model ($\gamma_t = 2949.7 - 10.9t$) and the negative value of the MK statistic, both of which suggest a clear downward trend in the x-series at the station. As a general rule, it may be concluded that the larger the MK statistic, the stronger the effect of time covariate on non-stationarity in the location parameter (Bazrafshan and Hejabi 2018).

Fig. 5 compares the number of times that the five covariates were used in the optimal non-stationary models across the studied stations. ENSO had the highest frequency, and frequencies of NCP, t, NAO, and AO, were ranked in the next positions, respectively. Notice that the importance of t in the optimal non-stationary models was higher than NAO and AO. This result confirmed the findings of the other researchers (Golian et al. 2015, Nazemosadat and Cordery 2000, Nazemosadat and Ghasemi 2004) who emphasized the importance of ENSO on the precipitation pattern over Iran.

3.4. Comparison of SSPEI and NSPEI

3.4.1. Temporal Variations

The two drought indices SSPEI and NSPEI were calculated on a 12-month timescale at all stations of interest. The temporal behaviors of these two indices for the sample stations in the arid (Yazd), semi-arid (Tabriz), Mediterranean (Gorgan), and per-humid (Bandar Anzali) climates were compared, as shown in Fig. 6. According to the figure, there was a slight difference between the time series of SSPEI and NSPEI in the extreme climates (arid and very humid). In the other hand, there was not much coincidence between the two indices in the semi-arid and Mediterranean climates. Especially in Tabriz station (with semi-arid climate), this difference was large in the final and early parts of the record period relative to the middle part. The large difference between the results of the two indices at Tabriz station and to some extent, at Gorgan station, seems to be attributed to the central role of covariates in non-stationary models. Focusing on Tabriz station reveals that time covariate was the most important factor responsible for non-stationarity in all 12 sub-periods models. At Gorgan station, however, the time covariate had a key role in the models of three out of 12 sub-periods. In the other two stations (Bandar Anzali and Yazd), the time covariate was not included in the optimal non-stationary models and the climatic indices have not had much effect on the changes in the location parameter.

In-depth analyzes of the results of other stations showed (figure not presented) wherever the covariates had a clear impact on P and AED (the two components needed for the calculation of the indices), there was a substantial difference between SSPEI and NSPEI. As a result, the difference between the time series of SSPEI and NSPEI had no association with the stations' climate in the study area.

3.4.2. Assessment of Drought Severity and Duration

Temporal variations of drought/wet events in terms of duration and severity (for the drought index < 0) have been compared between SSPEI and NSPEI, as shown in Fig. 7 for all chosen stations during 1964 – 2014. On the basis of SSPEI, the figure clearly shows the occurrence of a wet period during the first half of 1990s and a drought period during 1998–2014 (except 2004) at about all stations of interest. However, according to NSPEI, the long-term drought period of 1998-2014 has been broken into several minor droughts and wet periods, especially after 2004. For the decades before 1990s, although a dominant pattern of drought/wet period is not seen in the figure, the drought events in the first decade of record period (about 1964–1974) and the wet events in the second and third decades (about 1975–1990) are more common. Therefore, two key points from the figure may be inferred: 1) NSPEI modifies the severity of drought events, especially the long-term drought period 1998–2014, and 2) NSPEI breaks the long-term drought/wet periods into several short-term periods. For example, at Abadan station (the station shown with the number 1), while SSPEI identifies a 17-year (1964–1980) wet period, NSPEI breaks this continuous wet period into several minor droughts and wet periods.

The drought severity-duration (S-D) relationships related to the two indices SSEPI and NSPEI at four stations representing arid, semi-arid, Mediterranean, and very humid climates and across the studied stations are presented in Fig. 8. According to the figure, moving from the arid climate (Fig. 8a) to per-humid (Fig. 8d), both the severity and duration of droughts

decrease. In addition, the slopes of the S-D relationships are reduced. In other words, for a given drought duration, the severity of drought in arid climates is higher than that in semi-arid, Mediterranean, and per-humid climates.

Comparison between SSPEI and NSPEI shows that the slope of S-D equations in the Yazd, Tabriz and Bandar Anzali stations for NSPEI is slightly larger than SSPEI, which is not statistically significant. In most stations, the slope of the S-D relationships for NSPEI is greater than SSPEI. Fig. 8e is drawn on the basis of all drought durations and severities obtained from all stations of interest. This figure shows that the slope of the S-D relationship for NSPEI is slightly larger than SSPEI. However, a comparison of the S-D values in the same figure shows that SSPEI reports more severe and prolonged droughts than NSPEI over the record period.

3.4.3. Frequency Analysis of Drought Classes

Fig. 9 shows the frequency of different drought and wet period classes for the two indices SSPEI and NSPEI in the sample stations representing different climates of Iran. As per this figure, there is a slight difference between SSPEI and NSPEI in terms of the frequency of drought/wet period classes in arid (Fig. 9a) and per-humid (Fig. 9d) climates, but in semi-arid (Fig. 9b) and Mediterranean (Fig. 9c) climates, these differences are quite obvious in some classes. For example, in the semi-arid station of Tabriz (Fig. 9b), the frequencies of severe and extreme classes (mild and moderate classes) of drought for NSPEI are higher (lower) than those for SSPEI, but in the Mediterranean station of Gorgan (Fig. 9c) the results are exactly in reverse (i.e. frequencies of severe and extreme classes (mild to moderate classes) of drought for NSPEI are lower (higher) than those for SSPEI). On the basis of the mean values and standard deviations of frequencies for each class obtained from the total studied stations (Fig. 9e), the frequency of extreme drought for NSPEI is higher than SSPEI.

However, the frequencies for mild, medium and severe drought classes of SSPEI are higher than those of NSPEI.

3.4.4. Spatiotemporal Analysis of Drought and Wet Events

The average, minimum, and maximum time series of SSPEI and NSPEI are displayed in Fig. 10, which are calculated across the studied stations based on the water-year (October-September) data. As shown in the figure, both indices have an upward trend from1964-1993 and a downward trend from 1994 onwards, with a more decreasing slope for SSPEI compared to NSPEI. While SSPEI identifies several drought periods including 1964-1966, 1969-1970, 1972-1973, 1988-1990, 1998-2003, and 2005-2014, NSPEI detects 1964-1966, 1969-1970, 1972, 1976-77, 1983, 1988-1990, 1998-2003, 2005, 2007-2008, and 2013 as drought periods. The similar drought periods were also reported in Bazrafshan's et al. (2017), based on the Iran precipitation data over the past hundred years. The important point is that the long-term drought period of 2005-2014 identified by SSPEI has been broken by NSPEI into three smaller drought periods, namely 2005, 2007-2008, and 2013. Fig. 10 also represents the percentage of the country drought-affected area in different months during the period of 1964-2014. The figure shows that percentage of drought-prone areas has increased during drought periods.

Fig. 11 displays the spatiotemporal distribution of SSPEI and NSPEI over Iran during the water years (October-September) of 1964/65-2013/14. As shown in the figure, the difference between SSPEI and NSPEI in some years is relatively high. Focusing on drought events, NSPEI monitored more intensive and extensive droughts than SSPEI, especially in 1965/66, 1969/70, and 1972/73. However, in 1998/99, 1999/2000, 2007/08, and 2010/11, the intensity and extent of droughts monitored by SSPEI is higher than NSPEI. Among them, the two water years 1998/99 and 2010/11 are significantly different in terms of the zonation maps of SSPEI and NSPEI. In 1998/99, while about the whole country suffers from drought hazard

based on SSPEI, the eastern half of the country experiences the above-normal conditions according to the NSPEI results. Considering the 2010/11, the difference between the maps of SSPEI and NSPEI is higher than 1998/99. On the basis of SSPEI, almost all regions of the country are affected by drought in 2010/11 while NSPEI monitored the above-normal conditions in the majority of the country in the same year.

3.4.5. The Vegetation Response to the Drought Indicators

Applicability of remote sensing data (such as NDVI and VCI) for drought monitoring in Iran has been considered by several researchers (Rahimzadeh Bajgiran et al. 2008, Shamsipour et al. 2008). The results of the studies conducted in Iran showed that the temporal and spatial characteristics of drought could be detected and mapped using the indices derived from the satellite images.

In this study, the response of vegetation cover to the severest drought (the 2008 drought) monitored by SSPEI (as the base/traditional drought index) was investigated and compared to NSPEI. The monthly averages of VCI, SSPEI, and NSPEI throughout the studied stations were calculated for the period of September 2007 to November 2009, as displayed in Fig. 12. As shown in the figure, VCI identified a dry period in vegetation from May 2008 to March 2009, with the lowest value 16% in November 2008. The ground-based drought indices (SSPEI and NSPEI) simultaneously discerned a dry period beginning from February 2008, about three months prior that the satellite-based drought index (VCI) reports it. Although the two indicators were almost identical in terms of identifying the onset of the 2008 drought, they differed with regard to the characteristics such as the length of the drought period, the intensity and time of the drought peak, and the termination of the drought event. Especially in respect of the latter case, SSPEI does not seem to reach the above normal condition even several months after the drought termination identified by NSPEI and VCI. After the drought termination, both VCI and NSPEI remain above the normal condition, but

SSPEI is still below the normal condition. On the other hand, in November 2008, when VCI is in its lowest value, NSPEI detects a moisture signal which is very stronger than that of SSPEI. Four months later, VCI returns to normal in response to the signal. Thus, one can conclude the superiority of NSPEI, as a better indicator of vegetation response to meteorological drought than SSPEI, and the necessity for the development of non-stationary indicators for reliable and robust estimation of drought events.

4. Conclusion

In this study, a Non-stationary Standardized Precipitation Evapotranspiration Index (NSPEI) was developed for reliable and robust monitoring of meteorological drought characteristics in a changing environment. The NSPEI introduces a non-stationary, instead of stationary, log-logistic probability distribution in the mathematical structure of traditional SPEI (i.e. SSPEI). A non-stationary distribution assumes that its location parameter is a multivariate function of external covariates including time and several climate indices. The optimal non-stationary function was determined using a forward selection method in the framework of Generalized Additive Models in Location, Scale and Shape (GAMLSS) algorithm. The NSPEI was constructed at 32 weather stations across Iran for the period of 1964-2014. The proposed NSPEI was compared to SSPEI from different aspects. The key findings of this study are:

- Due to the significant decreasing trends in precipitation (P) and the significant increasing trends in atmospheric evaporative demand (AED) at most stations of interest, the water stress has intensified in Iran during last four decades up until 2014.
- The non-stationary log-logistic distribution fitted the water deficits/surpluses series (i.e. the P *minus* AED series) better than the stationary log-logistic distribution at almost all chosen stations.
- The location parameter of non-stationary log-logistic distribution mostly influenced by the two teleconnections ENSO and NCP. The time covariate had a more relative

importance than the other two teleconnections (i.e. NAO and AO) in simulating the temporal variations of location parameter.

- Existing the significant temporal trends in the P *minus* AED series led to the major differences between the NSPEI and SSPEI series at several stations. However, fluctuations of the two indicators were almost the same at those stations.
- The SSPEI monitored the drought events with durations and severities larger than those identified by NSPEI. Also, the long-term drought periods (e.g. the 1998/99-2013/14 droughts except 2004/05) quantified by SSPEI, were broken into the several discrete drought periods when using NSPEI.
- NSPEI identified the frequency of the extreme drought and wet events greater than SSPEI across the studied stations.
- There were clear differences between SSPEI and NSPEI in terms of the spatial maps of drought/wet events during the record period of 1964-2014.
- During the severest 2008 drought, the temporal variations of the average vegetation cover (quantified by average VCI) over the studied stations were closely related to those of the average NSPEI than the average SSPEI. NSPEI successfully identified the 2008 drought characteristics in vegetation cover in terms of both the drought duration and termination.

Acknowledgement

The authors would like to thank the Iran National Science Foundation (INSF) for funding this research under Grant Number 96010915. I also acknowledge I.R. of Iran Meteorological Organization for providing some data used in this study.

Ethical Approval

Not applicable.

Consent to Participate

Not applicable.

Consent to Publish

Not applicable.

Authors Contributions

Javad Bazrafshan: Conceptualization, Methodology, and Writing-Original draft preparation. **Majid Cheraghalizadeh**: Data curation, Methodology, Investigation and Editing, Visualization, Software, and Validation. **Kokab Shahgholian**: Investigation and Editing.

Funding

This study was funded by Iran National Science Foundation (Grant Number 96010915).

Competing Interests

The authors declare that they have no conflict of interest.

Availability of data and materials

Readers can contact authors for availability of data and materials.

References

Abramowitz, M. and Stegun, I.A. (1965) Handbook of mathematical functions with formulas, graphs, and mathematical tables, Dover Books on Advanced Mathematics, New York: Dover.

Akaike, H. (1974) A new look at the statistical model identification. IEEE Transactions on Automatic Control 19(6), 716-723.

Alizadeh-Choobari, O., Adibi, P. and Irannejad, P. (2018) Impact of the El Niño–Southern Oscillation on the climate of Iran using ERA-Interim data. Climate Dynamics 51(7), 2897-2911.

Allen, R.G., Pereira, L.S., Raes, D. and Smith, M. (1998) Crop Evapotranspiration. Guidelines for Computing Crop Water Requirements, p. 300p.

Asadi Zarch, M.A., Sivakumar, B. and Sharma, A. (2015) Droughts in a warming climate: A global assessment of Standardized precipitation index (SPI) and Reconnaissance drought index (RDI). Journal of Hydrology 526, 183-195.

Bateni, M.M., Behmanesh, J., Michele, C.D., Bazrafshan, J. and Rezaie, H. (2018) Composite Agrometeorological Drought Index Accounting for Seasonality and Autocorrelation. Journal of Hydrologic Engineering 23(6), 04018020.

Bazrafshan, J. (2017) Effect of Air Temperature on Historical Trend of Long-Term Droughts in Different Climates of Iran. Water Resources Management.

Bazrafshan, J. and Hejabi, S. (2018) A Non-Stationary Reconnaissance Drought Index (NRDI) for Drought Monitoring in a Changing Climate. Water Resources Management 32(8), 2611-2624.

Bazrafshan, J., Hejabi, S. and Eslamian, S. (2017) Handbook of Drought and Water Scarcity S., E. and F., E. (eds), pp. 167-188, Francis and Taylor, CRC Press, USA.

Bazrafshan, J., Hejabi, S. and Rahimi, J. (2014) Drought Monitoring Using the Multivariate Standardized Precipitation Index (MSPI). Water Resources Management 28(4), 1045-1060.

Beguería, S., Vicente-Serrano, S.M., Reig, F. and Latorre, B. (2014) Standardized precipitation evapotranspiration index (SPEI) revisited: parameter fitting, evapotranspiration models, tools, datasets and drought monitoring. International Journal of Climatology 34(10), 3001-3023.

Bhardwaj, K., Shah, D., Aadhar, S. and Mishra, V. (2020) Propagation of meteorological to hydrological droughts in India. Journal of Geophysical Research: Atmospheres n/a(n/a), e2020JD033455.

Burnham, K.P. and Anderson, D.R. (2002) Model selection and multimodel inference: A practical information-theoretical approach, Springer, New York.

Byun, H.-R. and Wilhite, D.A. (1999) Objective Quantification of Drought Severity and Duration. Journal of Climate 12(9), 2747-2756.

Cheng, L. and AghaKouchak, A. (2014) Nonstationary Precipitation Intensity-Duration-Frequency Curves for Infrastructure Design in a Changing Climate. Scientific Reports 4, 7093.

De Planhol, X. (2012) Famines, in: Encyclopedia Iranica, IX/2, pp. 203–206.

Dezfuli, A.K., Karamouz, M. and Araghinejad, S. (2010) On the relationship of regional meteorological drought with SOI and NAO over southwest Iran. Theoretical and Applied Climatology 100(1), 57-66.

Edossa, D.C., Woyessa, Y.E. and Welderufael, W.A. (2014) Analysis of Droughts in the Central Region of South Africa and Their Association with SST Anomalies. International Journal of Atmospheric Sciences 2014, 508953.

Ghaleb, F., Mario, M. and Sandra, A.N. (2015) Regional Landsat-Based Drought Monitoring from 1982 to 2014. Climate 3(3), 563-577.

Ghasemi, A.R. and Khalili, D. (2006) The influence of the Arctic Oscillation on winter temperatures in Iran. Theoretical and Applied Climatology 85(3), 149-164.

Ghasemi, A.R. and Khalili, D. (2008) The effect of the North Sea-Caspian pattern (NCP) on winter temperatures in Iran. Theoretical and Applied Climatology 92(1), 59-74.

Golian, S., Mazdiyasni, O. and AghaKouchak, A. (2015) Trends in meteorological and agricultural droughts in Iran. Theoretical and Applied Climatology 119(3), 679-688.

Guenang, G.M. and Kamga, F.M. (2014) Computation of the Standardized Precipitation Index (SPI) and Its Use to Assess Drought Occurrences in Cameroon over Recent Decades. Journal of Applied Meteorology and Climatology 53(10), 2310-2324.

Hamed, K.H. and Ramachandra Rao, A. (1998) A modified Mann-Kendall trend test for autocorrelated data. Journal of Hydrology 204(1), 182-196.

Hernandez, E.A. and Uddameri, V. (2014) Standardized precipitation evaporation index (SPEI)-based drought assessment in semi-arid south Texas. Environmental Earth Sciences 71(6), 2491-2501.

Hosking, J.R.M. (1990) L-Moments: Analysis and Estimation of Distributions Using Linear Combinations of Order Statistics. Journal of the Royal Statistical Society. Series B (Methodological) 52(1), 105-124.

Huang, S., Li, P., Huang, Q., Leng, G., Hou, B. and Ma, L. (2017) The propagation from meteorological to hydrological drought and its potential influence factors. Journal of Hydrology 547, 184-195.

IPCC (2014) Climate Change 2014: Synthesis Report. Contribution of Working Groups I, II and III to the Fifth Assessment Report of the Intergovernmental Panel on Climate Change [Core Writing Team, R.K. Pachauri and L.A. Meyer (eds.)]. IPCC, Geneva, Switzerland, 151 pp.

Kang, L. and Jiang, S. (2019) Bivariate Frequency Analysis of Hydrological Drought Using a Nonstationary Standardized Streamflow Index in the Yangtze River. Journal of Hydrologic Engineering 24(2), 05018031.

Kendall, M.G. (1970) Rank Correlation Methods, Griffin: London.

Khalili, A. (1997) Synthesis proceeding of integrated water plan of Iran. Jamab Consulting Engineering Co., Climate Section, The Ministry of Energy, Tehran, Iran.

Khalili, A. and Rahimi, J. (2014) High-resolution spatiotemporal distribution of precipitation in Iran: a comparative study with three global-precipitation datasets. Theoretical and Applied Climatology 118(1), 211-221.

Khalili, A. and Rahimi, J. (2018) The Soils of Iran. Roozitalab, M.H., Siadat, H. and Farshad, A. (eds), pp. 19-33, Springer International Publishing, Cham.

Kogan, F.N. (1995) Application of vegetation index and brightness temperature for drought detection. Advances in Space Research 15(11), 91-100.

Kwon, H.-H. and Lall, U. (2016) A copula-based nonstationary frequency analysis for the 2012–2015 drought in California. Water Resources Research 52(7), 5662-5675.

Li, J.Z., Wang, Y.X., Li, S.F. and Hu, R. (2015) A Nonstationary Standardized Precipitation Index incorporating climate indices as covariates. Journal of Geophysical Research: Atmospheres 120(23), 12,082-012,095.

Mann, H.B. (1945) Nonparametric Tests Against Trend. Econometrica 13(3), 245-259.

Mavromatis, T. (2007) Drought index evaluation for assessing future wheat production in Greece. International Journal of Climatology 27(7), 911-924.

McKee, T.B., Doeskin, N.J. and Kleist, J. (1993) The relationship of drought frequency and duration to time scales, pp. 179–184, American Meteorological Society, Anaheim, CA.

Mishra, A.K. and Singh, V.P. (2010) A review of drought concepts. Journal of Hydrology 391(1), 202-216.

Moradi, H.R. (2004) North atlantic oscilation index and its effect on climate of Iran. Geographical Research Quaterly 36(48), 17-30.

Nazemosadat, M.J. and Cordery, I. (2000) On the relationships between ENSO and autumn rainfall in Iran. International Journal of Climatology 20(1), 47-61.

Nazemosadat, M.J. and Ghasemi, A.R. (2004) Quantifying the ENSO-Related Shifts in the Intensity and Probability of Drought and Wet Periods in Iran. Journal of Climate 17(20), 4005-4018.

OFDA/CRED (2015) International Disaster Database. Université catholique de Louvain-BrusselsBelgium. http://www.emdat.be.

Paulo, A.A. and Pereira, L.S. (2006) Drought Concepts and Characterization. Water International 31(1), 37-49.

Pinzon, J.E. and Tucker, C.J. (2014) A Non-Stationary 1981–2012 AVHRR NDVI3g Time Series. Remote Sensing 6(8), 6929-6960.

Rahimi, J., Ebrahimpour, M. and Khalili, A. (2013) Spatial changes of Extended De Martonne climatic zones affected by climate change in Iran. Theoretical and Applied Climatology 112(3), 409-418.

Rahimzadeh Bajgiran, P., Darvishsefat, A.A., Khalili, A. and Makhdoum, M.F. (2008) Using AVHRR-based vegetation indices for drought monitoring in the Northwest of Iran. Journal of Arid Environments 72(6), 1086-1096.

Rashid, M.M. and Beecham, S. (2019) Development of a non-stationary Standardized Precipitation Index and its application to a South Australian climate. Science of The Total Environment 657, 882-892.

Raziei, T., Saghafian, B., Paulo, A.A., Pereira, L.S. and Bordi, I. (2008) Spatial Patterns and Temporal Variability of Drought in Western Iran. Water Resources Management 23(3), 439.

Rigby, R.A. and Stasinopoulos, D.M. (2005) Generalized additive models for location, scale and shape. Journal of the Royal Statistical Society: Series C (Applied Statistics) 54(3), 507-554.

Russo, S., Dosio, A., Sterl, A., Barbosa, P. and Vogt, J. (2013) Projection of occurrence of extreme dry-wet years and seasons in Europe with stationary and nonstationary Standardized Precipitation Indices. Journal of Geophysical Research: Atmospheres 118(14), 7628-7639.

Sattari, M.-T., Rezazadeh-Joudi, A. and Kusiak, A. (2017) Assessment of different methods for estimation of missing data in precipitation studies. Hydrology Research 48(4), 1032-1044.

Schwarz, G. (1978) Estimating the Dimension of a Model. The Annals of Statistics 6(2), 461-464.

Sen, P.K. (1968) Estimates of the Regression Coefficient Based on Kendall's Tau. Journal of the American Statistical Association 63(324), 1379-1389.

Şen, Z. (2015) Applied Drought Modeling, Prediction, and Mitigation, pp. 205-274, Elsevier, Boston.

Serinaldi, F. and Kilsby, C.G. (2015) Stationarity is undead: Uncertainty dominates the distribution of extremes. Advances in Water Resources 77, 17-36.

Shamsipour, A.A., AlaviPanah, S.K., Mohammadi, H., Azizi, A. and Khoshakhlagh, F. (2008) An analysis of drought events for central plains of Iran through an employment of NOAA-AVHRR data. Desert 13(2), 105-115.

Stasinopoulos, D.M., Rigby, R.A. and Akantziliotou, C. (2008) Instructions on how to use the GAMLSS package in R, 2nd edn. STORM Research Centre, London Metropolitan University, London.

Thornthwaite, C.W. (1948) An Approach toward a Rational Classification of Climate. Geographical Review 38(1), 55-94.

Tirivarombo, S., Osupile, D. and Eliasson, P. (2018) Drought monitoring and analysis: Standardised Precipitation Evapotranspiration Index (SPEI) and Standardised Precipitation Index (SPI). Physics and Chemistry of the Earth, Parts A/B/C 106, 1-10.

Vaghefi, S.A., Keykhai, M., Jahanbakhshi, F., Sheikholeslami, J., Ahmadi, A., Yang, H. and Abbaspour, K.C. (2019) The future of extreme climate in Iran. Scientific Reports 9(1), 1464-1464.

Van Lanen, H.A.J. (2006) Drought propagation through the hydrological cycle. Demuth, S., Gustard, A., Planos, E., Scatena, F. and Servat, E. (eds), pp. 122–127, IAHS Press, Wallingford, UK.

Van Loon, A.F. (2015) Hydrological drought explained. Wiley Interdisciplinary Reviews: Water 2(4), 359-392.

Vicente-Serrano, S.M., Beguería, S. and López-Moreno, J.I. (2010) A Multiscalar Drought Index Sensitive to Global Warming: The Standardized Precipitation Evapotranspiration Index. Journal of Climate 23(7), 1696-1718.

Wang, Y., Duan, L., Liu, T., Li, J. and Feng, P. (2020) A Non-stationary Standardized Streamflow Index for hydrological drought using climate and human-induced indices as covariates. Science of The Total Environment 699, 134278.

Wang, Y., Li, J., Feng, P. and Hu, R. (2015) A Time-Dependent Drought Index for Non-Stationary Precipitation Series. Water Resources Management 29(15), 5631-5647.

Wilhite, D.A. (2000) Drought: A Global Assessment,, Routledge, London.

Wilhite, D.A. and Glantz, M.H. (1985) Understanding: the Drought Phenomenon: The Role of Definitions. Water International 10(3), 111-120.

WMO (2012) Standardized Precipitation Index User Guide, Geneva.

Yue, S., Pilon, P., Phinney, B. and Cavadias, G. (2002) The influence of autocorrelation on the ability to detect trend in hydrological series. Hydrological Processes 16(9), 1807-1829.

Zarei, A.R. and Mahmoudi, M.R. (2020) Assessment of the effect of PET calculation method on the Standardized Precipitation Evapotranspiration Index (SPEI). Arabian Journal of Geosciences 13(4), 182.

Tables:

Table 1. Geographic and climatic characteristics of the chosen weather stations.

#. Station's name	Longitude (degree)	Latitude (degree)	Elevation (m)	Long-term Annual Mean of		Climate
				Precipitation (mm)	Air Temperature (ºC)	
1. Abadan	48.25	30.37	6.6	152.2	25.6	Arid
2. Ahwaz	48.67	31.33	22.5	224.6	26.2	Arid
3. Arak	49.77	34.10	1708	328.6	13.8	Semi-arid
4. Bam	58.35	29.10	1066.9	58.1	23.4	Arid
5. Bandar Abbas	56.37	27.22	9.8	169.8	27.1	Arid
6. Bandar Anzali	49.45	37.48	-23.6	1774.4	16.3	Very Humid
7. Birjand	59.20	32.87	1491	162.0	16.8	Arid
8. Bushehr	50.82	28.97	9.0	243.3	24.8	Arid
9. Esfahan	51.67	32.62	1550.4	125.1	16.5	Arid
10. Gazvin	50.05	36.25	1279.2	317.9	14.2	Semi-arid
11. Gorgan	54.40	36.90	0.0	575.8	17.7	Mediterranean
12. Kerman	56.97	30.25	1753.8	138.5	17.1	Arid
13. Kermanshah	47.15	34.35	1318.6	444.8	14.9	Semi-arid
14. Khorramabad	48.28	33.43	1147.8	493.5	17.3	Semi-arid
15. Khoy	44.97	38.55	1103	292.2	12.6	Semi-arid
16. Mashhad	59.63	36.27	999.2	250.4	14.4	Semi-arid
17. Oroomieh	45.05	37.67	1328	330.0	11.1	Semi-arid
18. Ramsar	50.67	36.91	-20.0	1216.3	16.1	Very Humid
19. Rasht	49.62	37.32	-8.6	1338.7	16.2	Very Humid
20. Sabzevar	57.65	36.20	972.0	189.4	17.7	Arid
21. Saghez	46.27	36.25	1522.8	483.9	12.0	Semi-arid
22. Sanandaj	47.00	35.33	1373.4	443.8	14.2	Semi-arid
23. Shahrekord	50.85	32.28	2048.9	331.1	12.3	Semi-arid
24. Shahroud	54.95	36.42	1349.1	157.1	14.8	Arid
25. Shiraz	52.60	29.53	1484.0	317.5	18.1	Semi-arid
26. Tabriz	46.28	38.08	1361.0	282.3	12.4	Semi-arid
27. Tehran Mehrabad	51.32	35.68	1190.8	234.0	17.5	Arid
28. Torbat Heydarieh	59.22	35.27	1450.8	259.5	14.7	Semi-arid
29. Yazd	54.28	31.90	1237.2	56.5	19.6	Arid
30. Zabol	61.48	31.03	489.2	55.8	22.6	Arid
31. Zahedan	60.88	29.47	1370.0	80.2	18.7	Arid
32. Zanjan	48.48	36.68	1663.0	308.0	11.4	Semi-arid

Table 2. Description of the SSPEI/NSPEI classes (Edossa et al. 2014).

SSPEI/NSPEI Classes	Description
≥ 2.00	Extreme wet
1.50 to 1.99	Severe wet
1.00 to 1.49	Moderate wet
0.00 to 0.99	Mild wet
-0.99 to 0.00	Mild drought
-1.00 to -1.49	Moderate drought
-1.50 to -1.99	Severe drought
≤ -2.00	Extreme drought

Table 3. The Mann-Kendall (MK) statistics, their corresponding p-values, and the Sen's slope (SS) estimators for precipitation (P), atmospheric evaporative demand (AED), and D=P-AED at the stations of interest for 12-month timescale.

Station	**P**			**AED**			**D=P-AED**		
	MK	**p-value**	**SS (mm/decade)**	**MK**	**p-value**	**SS (mm/decade)**	**MK**	**p-value**	**SS (mm/decade)**
Abadan	0.20	0.840	0.01	16.67	0.000	9.15	-15.38	0.000	-9.07
Ahwaz	-2.27	0.020	-0.41	-5.25	0.000	-3.14	4.70	0.000	3.12
Arak	-7.73	0.000	-1.36	6.38	0.000	0.74	-8.07	0.000	-1.96
Bam	-3.70	0.000	-0.23	10.80	0.000	4.55	-11.02	0.000	-4.54
Bandar Abbas	-0.09	0.930	0.00	-6.49	0.000	-3.20	5.11	0.000	3.03
Bandar Anzali	-1.88	0.060	-1.26	12.32	0.000	1.27	-3.68	0.000	-2.49
Birjand	-3.23	0.000	-0.38	-4.58	0.000	-0.80	1.93	0.054	0.42
Bushehr	0.88	0.380	0.20	18.83	0.000	5.53	-13.09	0.000	-5.10
Esfahan	9.63	0.000	1.07	17.10	0.000	1.91	-5.15	0.000	-0.82
Gazvin	1.60	0.110	0.28	-12.09	0.000	-2.60	9.64	0.000	2.98
Gorgan	-11.38	0.000	-2.78	-9.31	0.000	-1.40	-4.29	0.000	-1.34
Kerman	-6.36	0.000	-0.57	-2.99	0.003	-0.73	1.66	0.097	0.44
Kermanshah	-8.36	0.000	-1.94	19.13	0.000	2.66	-14.10	0.000	-4.68
Khorramabad	-7.04	0.000	-1.89	-6.45	0.000	-2.12	1.30	0.195	0.51
Khoy	0.07	0.950	0.01	-0.43	0.665	-0.06	1.53	0.125	0.33
Mashhad	-1.07	0.280	-0.18	21.70	0.000	3.27	-12.46	0.000	-3.35
Oroomieh	-6.02	0.000	-1.15	3.98	0.000	0.43	-6.07	0.000	-1.60
Ramsar	-3.24	0.000	-1.98	13.22	0.000	1.75	-5.31	0.000	-3.48
Rasht	-2.72	0.010	-1.42	-6.73	0.000	-0.82	-0.74	0.457	-0.43
Sabzevar	1.52	0.130	0.21	-0.03	0.977	0.00	0.22	0.827	0.06
Saghez	-6.56	0.000	-1.73	-5.56	0.000	-0.57	-3.62	0.000	-1.21
Sanandaj	-10.11	0.000	-2.60	-11.03	0.000	-1.31	-4.12	0.000	-1.23
Shahrekord	0.91	0.360	0.18	-20.27	0.000	-3.32	13.07	0.000	3.43
Shahroud	-2.62	0.010	-0.28	-0.06	0.956	-0.01	-1.82	0.069	-0.32
Shiraz	1.12	0.260	0.30	21.77	0.000	3.26	-9.35	0.000	-3.06
Tabriz	-12.90	0.000	-2.06	16.91	0.000	1.67	-17.07	0.000	-3.94
Tehran (Mehrabad)	2.60	0.010	0.42	20.62	0.000	2.78	-10.12	0.000	-2.33
Torbat Heydarieh	-1.31	0.190	-0.25	-11.75	0.000	-2.02	6.30	0.000	1.65
Yazd	-1.10	0.270	-0.06	3.72	0.000	0.62	-3.82	0.000	-0.72
Zabol	-4.04	0.000	-0.26	6.17	0.000	2.26	-5.91	0.000	-2.52
Zahedan	-4.42	0.000	-0.34	20.08	0.000	3.17	-17.05	0.000	-3.52
Zanjan	-4.71	0.000	-0.79	-14.20	0.000	-2.19	6.24	0.000	1.34

Table 4. Forward selection of covariates for non-stationary modeling of the location parameter of log-logistic distribution for the 12-month sub-period of October-September. nAIC indicates the Akaike Information Criterion (AIC) for each step of the selection process of a non-stationary model. sAIC shows the AIC for the stationary assumption of the log-logistic distribution parameters.

Station	Selected variables in Forward Selection					nAIC					sAIC
	Step(1)	Step(2)	Step(3)	Step(4)	Step(5)	Step(1)	Step(2)	Step(3)	Step(4)	Step(5)	
Abadan	t	NCP(t-5)	AO(t-12)	NAO(t-9)	ENSO(t-12)	720*	**719.4**	721.0	722.8	724.6	743.3
Ahwaz	NAO(t-3)	ENSO(t-8)	AO(t-12)	NCP(t-10)	t	738.8	731.4*	730.2	**730.0**	731.5	748.6
Arak	ENSO(t)	t	NCP(t-3)	AO(t)	NAO(t)	649.2	647.4	646.7*	647.6	**645.3**	654.1
Bam	t	ENSO(t)	NAO(t-4)	NCP(t-1)	AO(t-7)	680.8	**678.6***	679.2	679.8	681.1	686.9
Bandar Abbas	NAO(t-12)	NCP(t)	t	ENSO(t)	AO(t-9)	706.9	699.8	697.5*	**697.2**	698.0	717.2
Bandar Anzali	ENSO(t)	NAO(t-11)	NCP(t)	AO(t-1)	t	755.9	753.5*	**752.3**	753.7	755.6	756.7
Birjand	ENSO(t-1)	AO(t-8)	NAO(t-9)	NCP(t-3)	t	616.6	611.9*	**610.0**	611.5	613.5	625.2
Bushehr	t	NCP(t-8)	ENSO(t)	AO(t-10)	NAO(t-12)	677.7	669.3*	**669.2**	670.1	670.4	693.8
Esfahan	NCP(t-9)	t	AO(t-8)	NAO(t-10)	ENSO(t)	**606.5***	606.9	607.9	608.4	609.5	608.4
Gazvin	ENSO(t-1)	t	AO(t-12)	NAO(t-8)	NCP(t-6)	655.5	650*	649.9	649.7	**648.7**	663.1
Gorgan	NCP(t-8)	ENSO(t-11)	t	AO(t-6)	NAO(t)	650.9	649.3	648.5	648.7	**645.6***	656.9
Kerman	t	ENSO(t-5)	NAO(t-7)	AO(t-5)	NCP(t-8)	**664.4**	665.1	665.4	664.4	666.2	644.1*
Kermanshah	ENSO(t)	NAO(t)	NCP(t-10)	AO(t-8)	t	**637.9***	638.0	639.3	640.4	642.4	684.1
Khorramabad	ENSO(t)	NCP(t-3)	NAO(t-12)	AO(t-10)	t	685.6*	**683.7**	683.9	684.2	685.9	693.2
Khoy	NCP(t-1)	ENSO(t)	NAO(t)	AO(t-1)	t	629.5*	628.9	629.4	**628.4**	629.5	633.7
Mashhad	t	ENSO(t)	NCP(t-2)	AO(t-8)	NAO(t-9)	652.4	645.3	642.3	641.9	**638.0***	664.7
Oroomieh	ENSO(t-5)	t	NCP(t-1)	NAO(t-9)	AO(t-10)	650.3	647.3	647.2	647.0	**644.5***	654.3
Ramsar	NCP(t)	ENSO(t)	NAO(t-6)	t	AO(t-8)	736.2	733.5*	**732.5**	733.0	733.3	742.6
Rasht	NCP(t-1)	ENSO(t)	NAO(t)	AO(t-1)	t	712.8	710.2*	709.9	**709.0**	710.9	724.6
Sabzevar	NCP(t-2)	ENSO(t)	NAO(t-5)	AO(t-8)	t	643.4	639.0	635.1*	**633.7**	635.3	650.6
Saghez	ENSO(t-1)	NCP(t-2)	AO(t-7)	NAO(t)	t	671.2*	671.2	**670.3**	671.5	673.2	683.8
Sanandaj	ENSO(t)	t	NAO(t-7)	NCP(t-3)	AO(t-1)	653.5	651.2	**647.0***	647.1	648.5	663.4
Shahrekord	t	ENSO(t)	NCP(t-3)	NAO(t-6)	AO(t-7)	642.3	632.7	627.4	627.1*	**625.2**	657.1
Shahroud	ENSO(t)	NCP(t-3)	AO(t-12)	NAO(t-10)	t	611.7	608.6*	**606.7**	607.8	609.3	617.3
Shiraz	t	ENSO(t)	AO(t-8)	NAO(t-6)	NCP(t-1)	673.2	668.5	667.0*	**666.4**	667.8	678.0
Tabriz	t	NCP(t-1)	NAO(t-7)	ENSO(t-1)	AO(t-5)	615.2	609.5	602.4	**595.1***	595.4	649.5
Tehran Mehrabad	t	NCP(t-9)	ENSO(t-5)	NAO(t-1)	AO(t-3)	629.9	624.6	623.7	623.9	**620.9***	636.5
Torbat Heydarieh	ENSO(t)	AO(t-8)	t	NCP(t-2)	NAO(t-5)	652.1	648.5*	**646.9**	647.3	648.4	657.1
Yazd	NAO(t-3)	NCP(t)	AO(t-8)	ENSO(t-12)	t	**636.2***	636.3	637.7	639.2	640.7	636.8
Zabol	NCP(t-2)	t	ENSO(t)	AO(t-12)	NAO(t-10)	664.5	659.9	657.6*	658.0	**657.1**	672.3
Zahedan	t	NCP(t-6)	ENSO(t-8)	NAO(t-5)	AO(t-5)	603.2	600.2*	**600.1**	601.1	600.1	632.4
Zanjan	ENSO(t-5)	NCP(t-2)	t	NAO(t-7)	AO(t-9)	620.6*	619.5	**619.2**	620.5	621.0	624.7

* indicates the optimal model, and the bolded numbers indicate the best model.

Table 5. The optimal non-stationary model fitted to the x-series of October-September for estimation of the location parameter ($\gamma(t)$) of log-logistic distribution at the stations of interest.

Station	**Optimal Non-stationary Model**		**MK Test**
	Location Parameter ($\gamma(t)$)	**AIC**	
Abadan	$2949.7 - 10.9t$	720.0	-4.84**
Ahwaz	$2306.5 + 368.6NAO(t-3) - 136.2ENSO(t-8)$	731.4	0.92
Arak	$4554.9 - 52.8ENSO(t) - 2.04\,t + 84.3NCP(t-3)$	646.7	-1.92*
Bam	$3440.3 - 4.1\,t - 61.1\,ENSO(t)$	678.6	-3.21**
Bandar Abbas	$2717.3 + 234.8\,NAO(t-12) + 308.6\,NCP(t) + 3.5\,t$	697.5	1.59
Bandar Anzali	$5856.6 - 140.5ENSO(t) - 253.5\,NAO(t-11)$	753.5	-0.94
Birjand	$4229.6 - 47.9\,ENSO(t-1) + 64.6\,AO(t-8)$	611.9	0.34
Bushehr	$3608.4 - 6.2\,t + 226.7\,NCP(t-8)$	669.3	-3.61**
Esfahan	$4182.4 + 71.4\,NCP(t-9)$	606.5	-1.08
Gazvin	$4408.3 - 71.8\,ENSO(t-1) + 3.1\,t$	650.0	2.39**
Gorgan	$4641.1 + 167.4\,NCP(t-8) - 34.3\,ENSO(t-11) - 1.1\,t - 127.6\,AO(t-6) + 119.4\,NAO(t)$	645.6	-2.20*
Kerman	$4202.2 + 0.12\,t$	664.4	-0.5
Kermanshah	$4588.1 - 38.1\,ENSO(t)$	637.9	-4.33**
Khorramabad	$4502.7 - 98.9\,ENSO(t)$	685.6	-0.15
Khoy	$4496.7 + 115.7\,NCP(t-1)$	629.5	-0.17
Mashhad	$4538.8 - 4.8\,t - 79.4\,ENSO(t) + 71.3\,NCP(t-2) + 147.0\,AO(t-8) - 130.7\,NAO(t-9)$	638.0	-3.18**
Oroomieh	$4702.6 - 62.7\,ENSO(t-5) - 2.7\,t + 48.5\,NCP(t-1) - 144.5\,NAO(t-9) + 115.5\,AO(t-10)$	644.5	-2.31*
Ramsar	$5341.2 + 335.0\,NCP(t) - 109.6\,ENSO(t)$	733.5	-1.43
Rasht	$5461.3 + 404.8\,NCP(t-1) - 95.9\,ENSO(t)$	710.2	-0.65
Sabzevar	$4103.9 + 181.6\,NCP(t-2) - 63.9\,ENSO(t) - 89.2\,NAO(t-5)$	635.1	0.32
Saghez	$4756.8 - 113.6\,ENSO(t-1)$	671.2	-1.52
Sanandaj	$4656.8 - 101.6\,ENSO(t) - 2.5\,t - 100.0\,NAO(t-7)$	647.0	-1.62
Shahrekord	$4451.3 + 4.9\,t - 74.4\,ENSO(t) + 147.0\,NCP(t-3) - 50.9\,NAO(t-6)$	627.1	3.75**
Shahroud	$4304.8 - 42.2\,ENSO(t) + 77.5\,NCP(t-3)$	608.6	-0.48
Shiraz	$4400.0 - 4.0\,t - 59.1\,ENSO(t) + 83.1\,AO(t-8)$	667.0	-2.31*
Tabriz	$4634.4 - 4.8\,t + 117.0\,NCP(t-1) - 99.5\,NAO(t-7) - 41.2\,ENSO(t-1)$	595.1	-5.33**
Tehran Mehrabad	$4244.7 - 2.1\,t + 93.4NCP(t-9) - 7.7\,ENSO(t-5) + 116.1\,NAO(t-1) - 101.7AO(t-3)$	620.9	-2.6**
Torbat Heydarieh	$4477.1 - 58.5\,ENSO(t) + 88.9\,AO(t-8)$	648.5	1.95*
Yazd	$3755.4 + 59.3\,NAO(t-3)$	636.2	-0.81
Zabol	$3548.3 + 258.6\,NCP(t-2) - 3.6\,t - 66.2\,ENSO(t)$	657.6	-1.71*
Zahedan	$4145.4 - 4.0\,t + 65.8\,NCP(t-6)$	600.2	-4.98**
Zanjan	$4602.9 - 34.6\,ENSO(t-5)$	620.6	1.19

[*] indicates the 5% significance level, and [**] indicates the 1% significance level.

Figures:

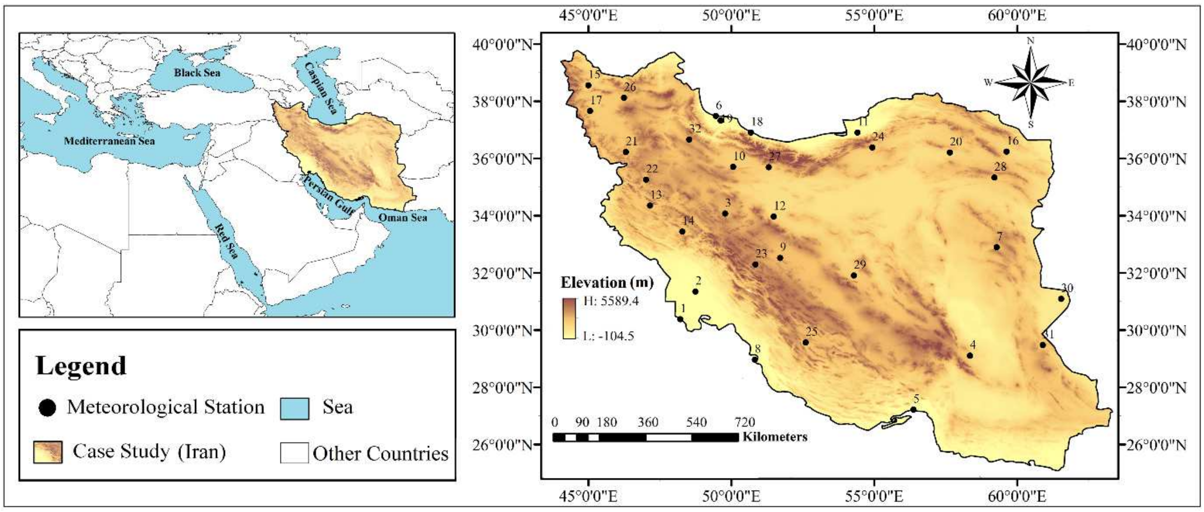

Fig. 1. Positions of the chosen weather stations in the study area, Iran. The stations numbers have been described in Table 1.

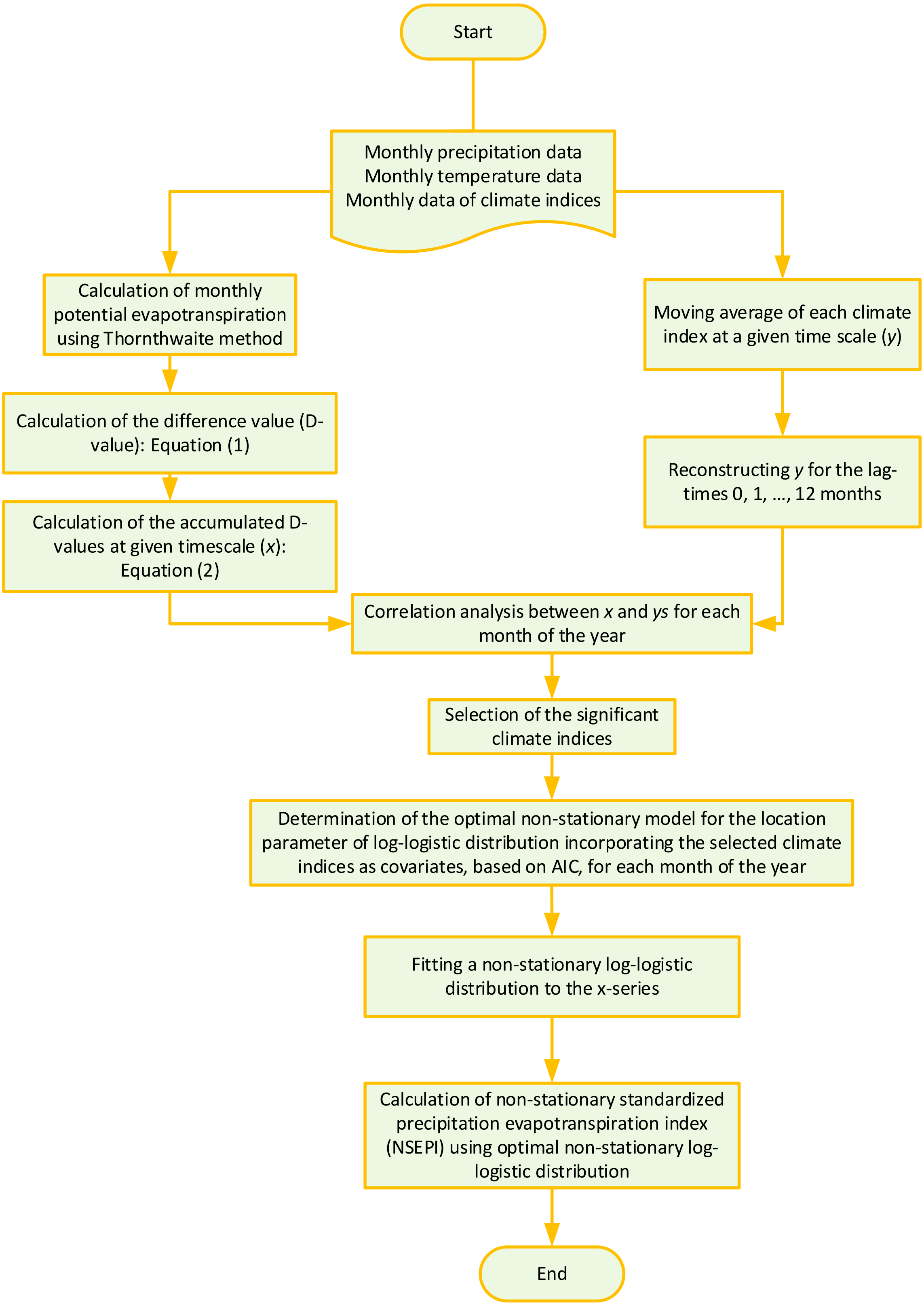

Fig. 2. Displaying the steps for calculation of NSPEI in this study

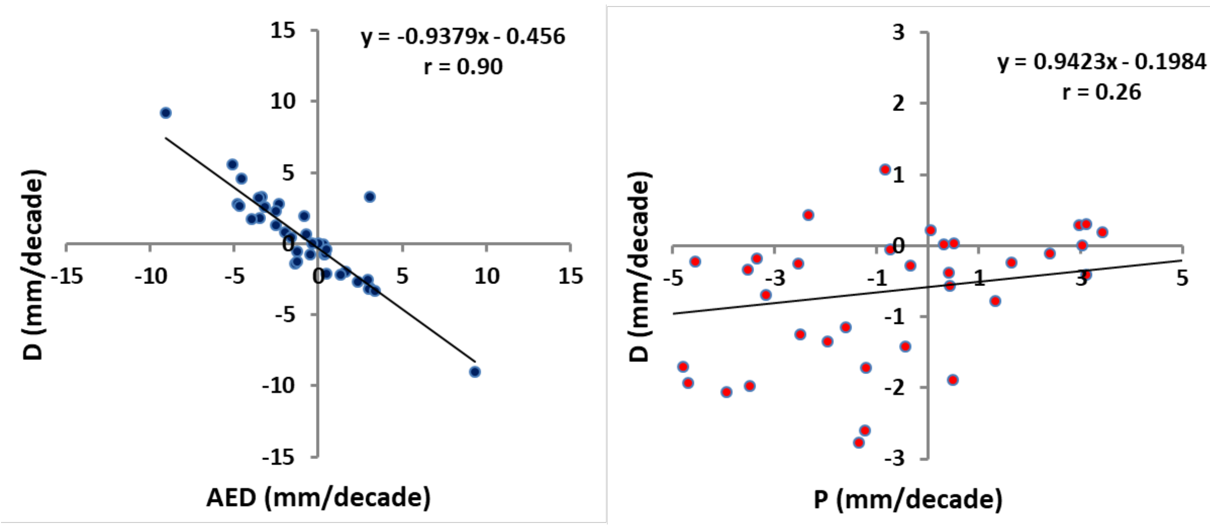

Fig. 3. The trend magnitudes in D *vs*. the trend magnitudes in AED (left panel) and the trend magnitudes in D *vs*. the trend magnitudes in P (right panel) across all chosen stations.

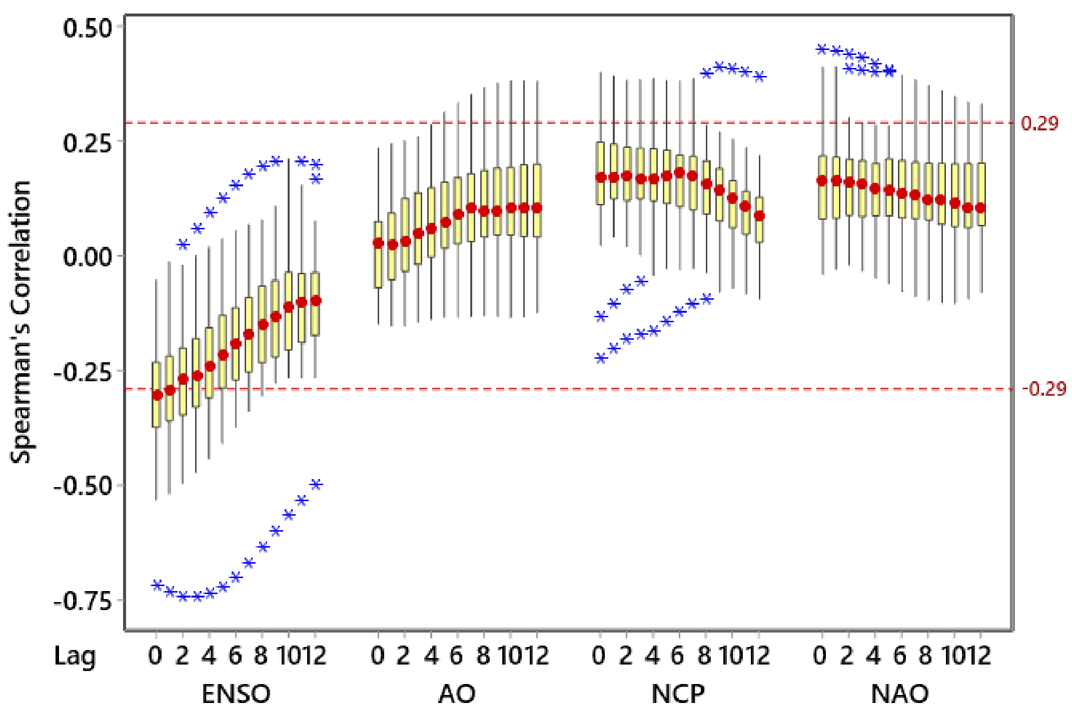

Fig. 4. Boxplot of the Spearman's correlation coefficients between D and each of the four selected climate indices (ENSO, AO, NCP, and NAO) in this study for the lag-times 0-12 months. Each box-whisker represents the 5^{th}, 25^{th}, 50^{th}, 75^{th}, and 95th percentiles across the stations and the outliers are indicated with the stars. The red dotted lines show the 95^{th} confidence interval of correlation coefficients.

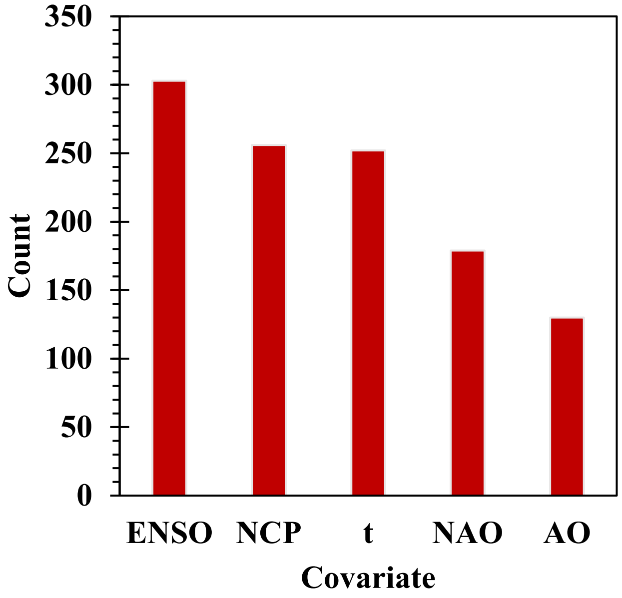

Fig. 5. Comparison of the five covariates in terms of the times used in the non-stationary models of the location parameter of log-logistic distribution across the stations of interest.

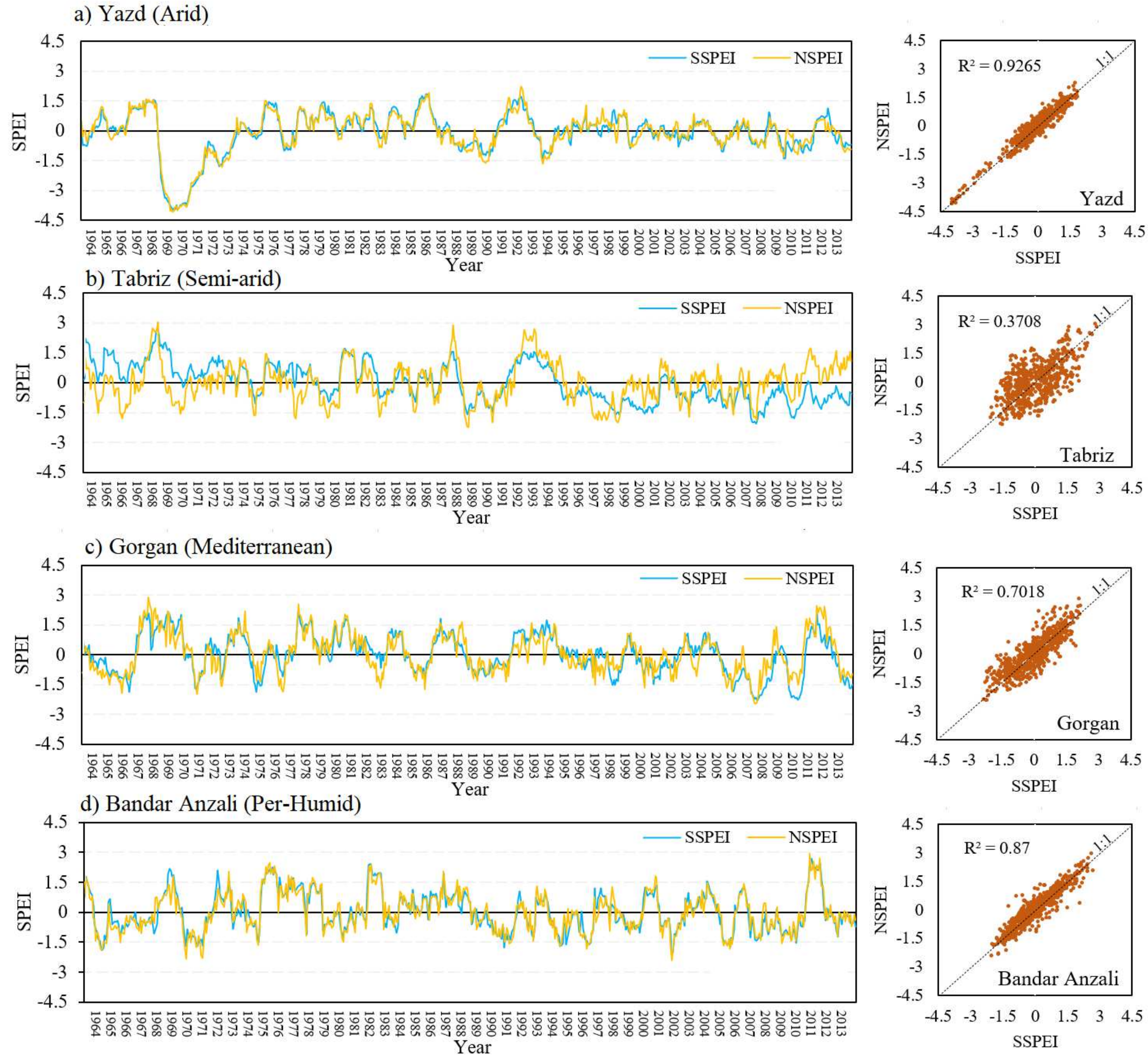

Fig. 6. Comparison of the SSPEI and NSPEI time series at the sample stations: a) Yazd, b) Tabriz, c) Gorgan, and d) Bandar Anzali. The right-side diagrams display the scatter plots of NSPEI vs. SSPEI at the same stations.

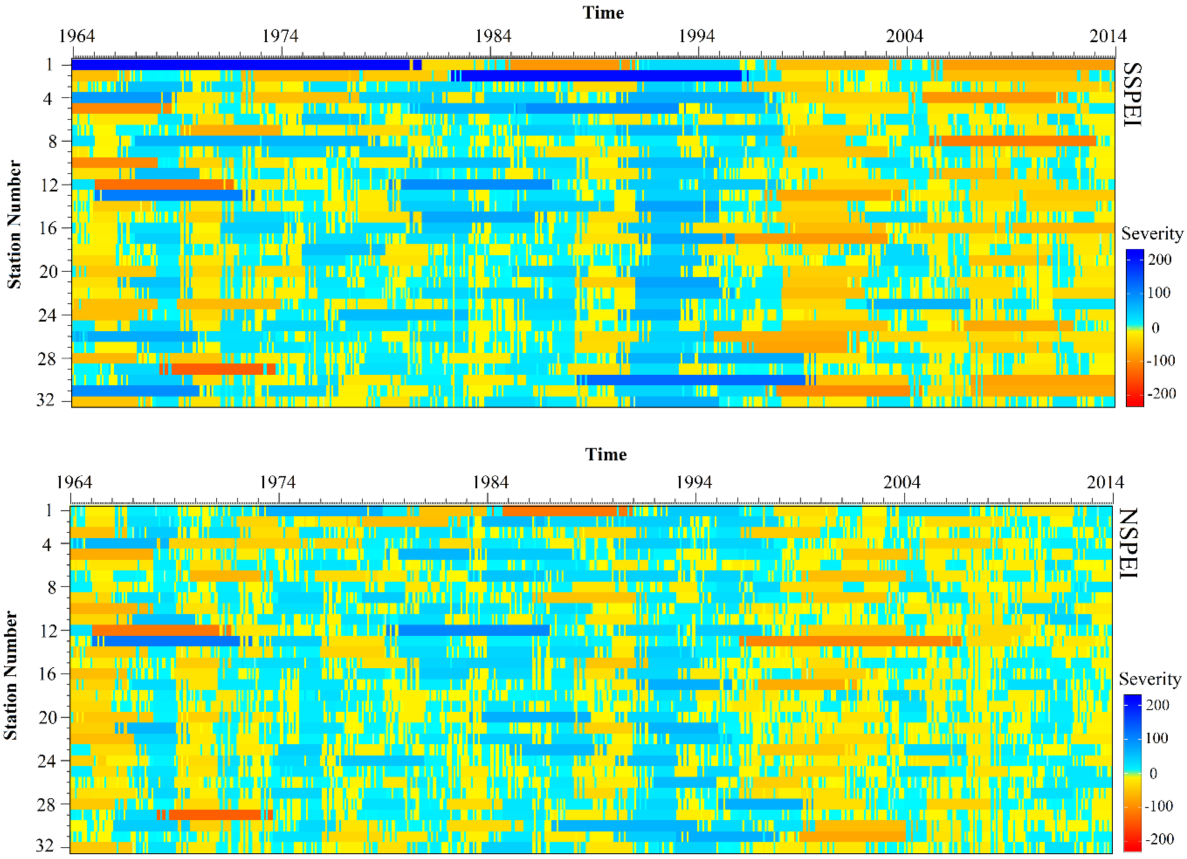

Fig. 7. Temporal variations of the drought/wet events durations and severities for the whole stations of interest during 1964-2014 based on SSPEI (upper) and NSPEI (lower).

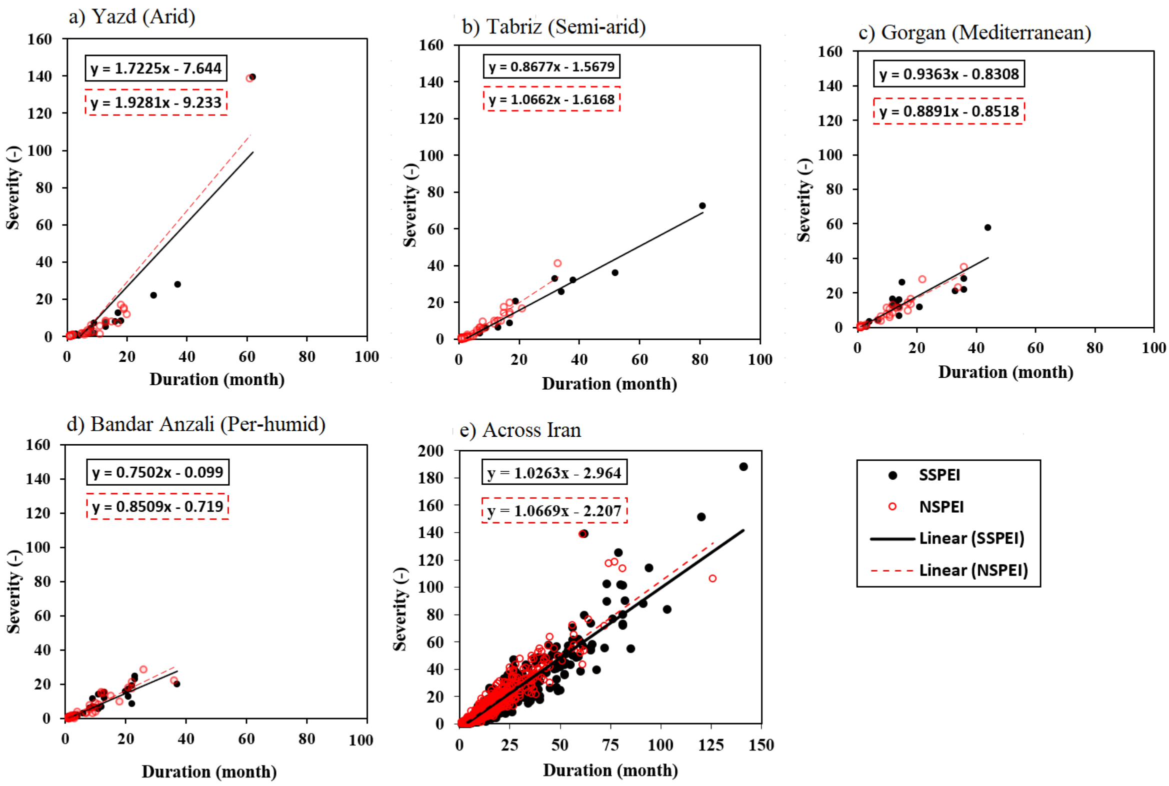

Fig. 8. The severity-duration relationships for SSPEI and NSPEI at the sample stations (a) Yazd, b) Tabriz, c) Gorgan, and d) Bandar Anzali), and across Iran (e).

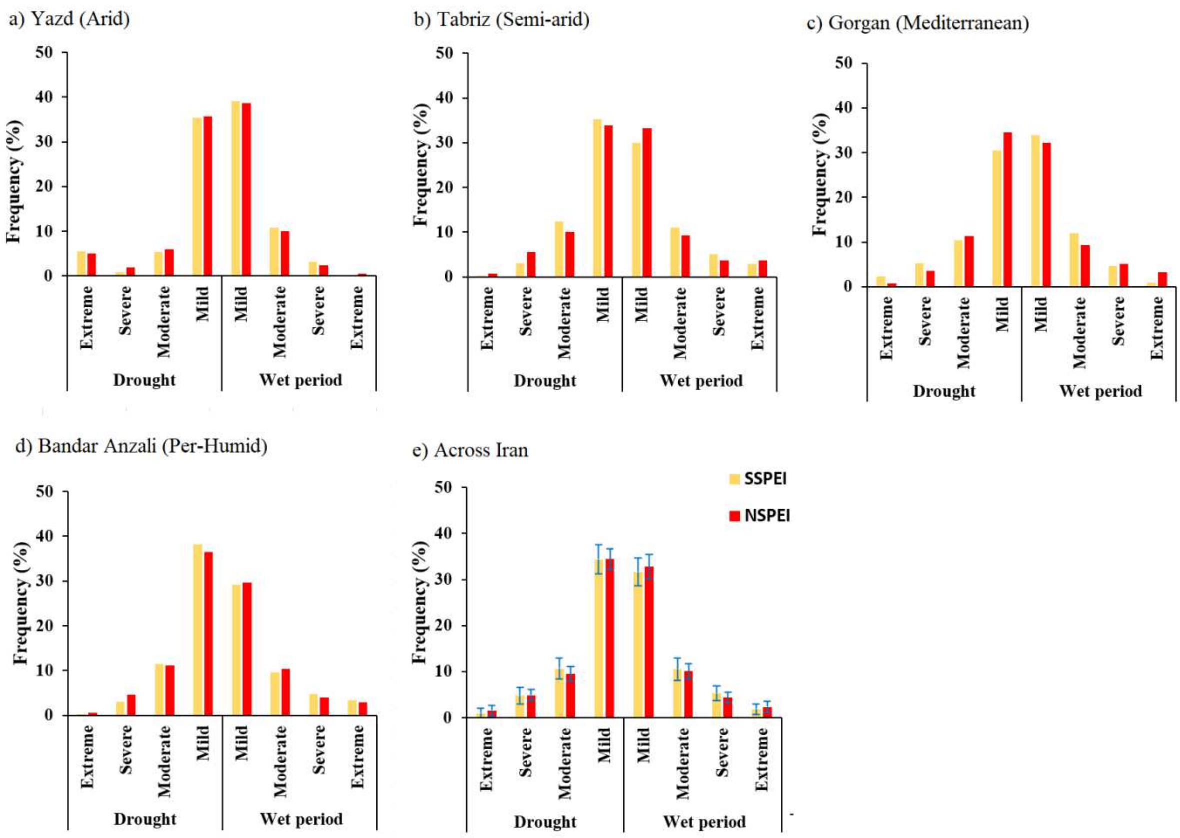

Fig. 9. Frequency of drought and wet period classes for SSPEI and NSPEI at the sample stations: a) Yazd, b) Tabriz, c) Gorgan, d) Bandar Anzali, and e) across Iran (bars show mean ± standard deviation across the stations).

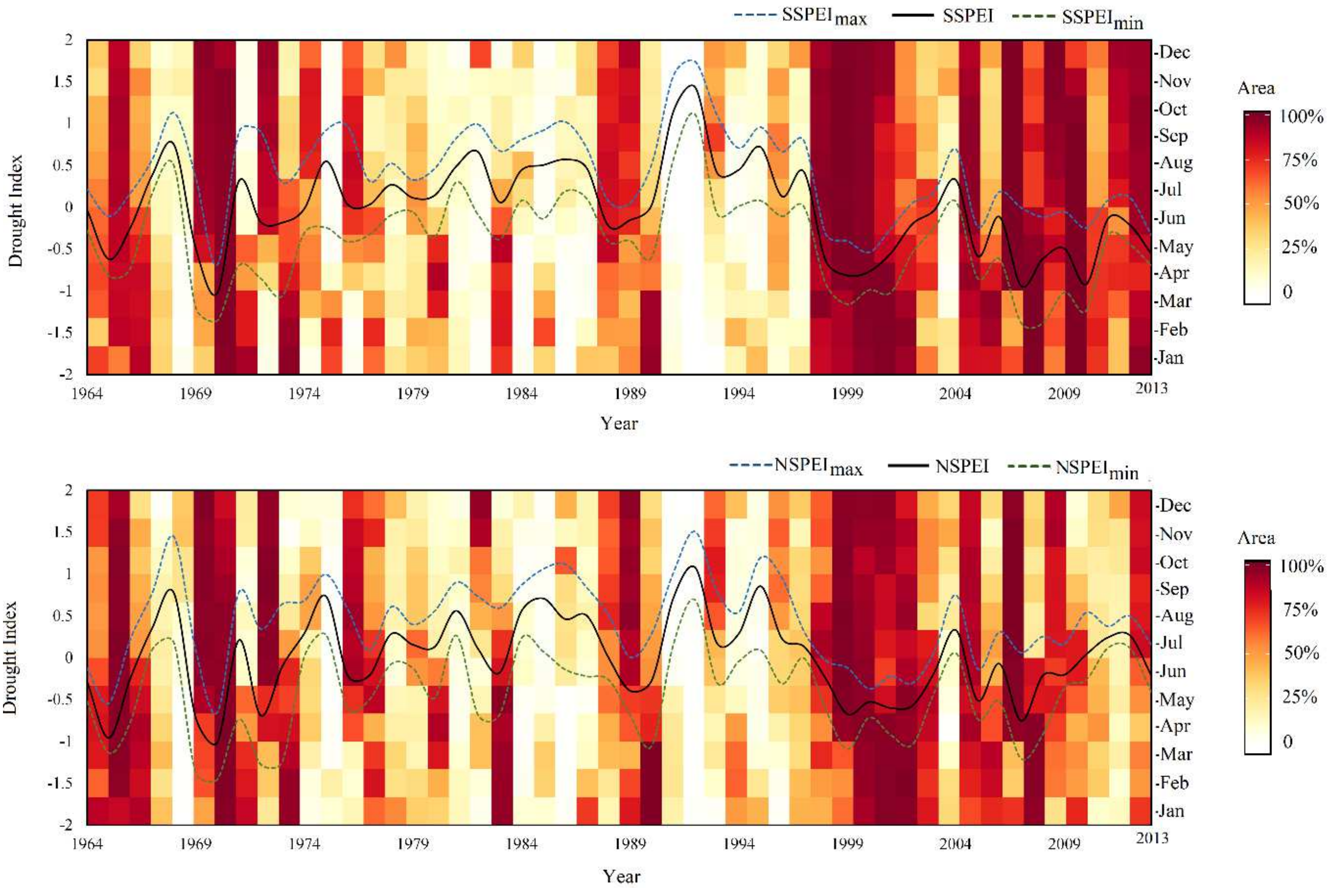

Fig. 10. The water-year (i.e. October-September) average, minimum, and maximum time series of SSEPI (upper) and NSPEI (lower) across the studied stations, accompanying the percentage areas of the country under drought conditions (drought index < 0) during 1964/65-2013/14.

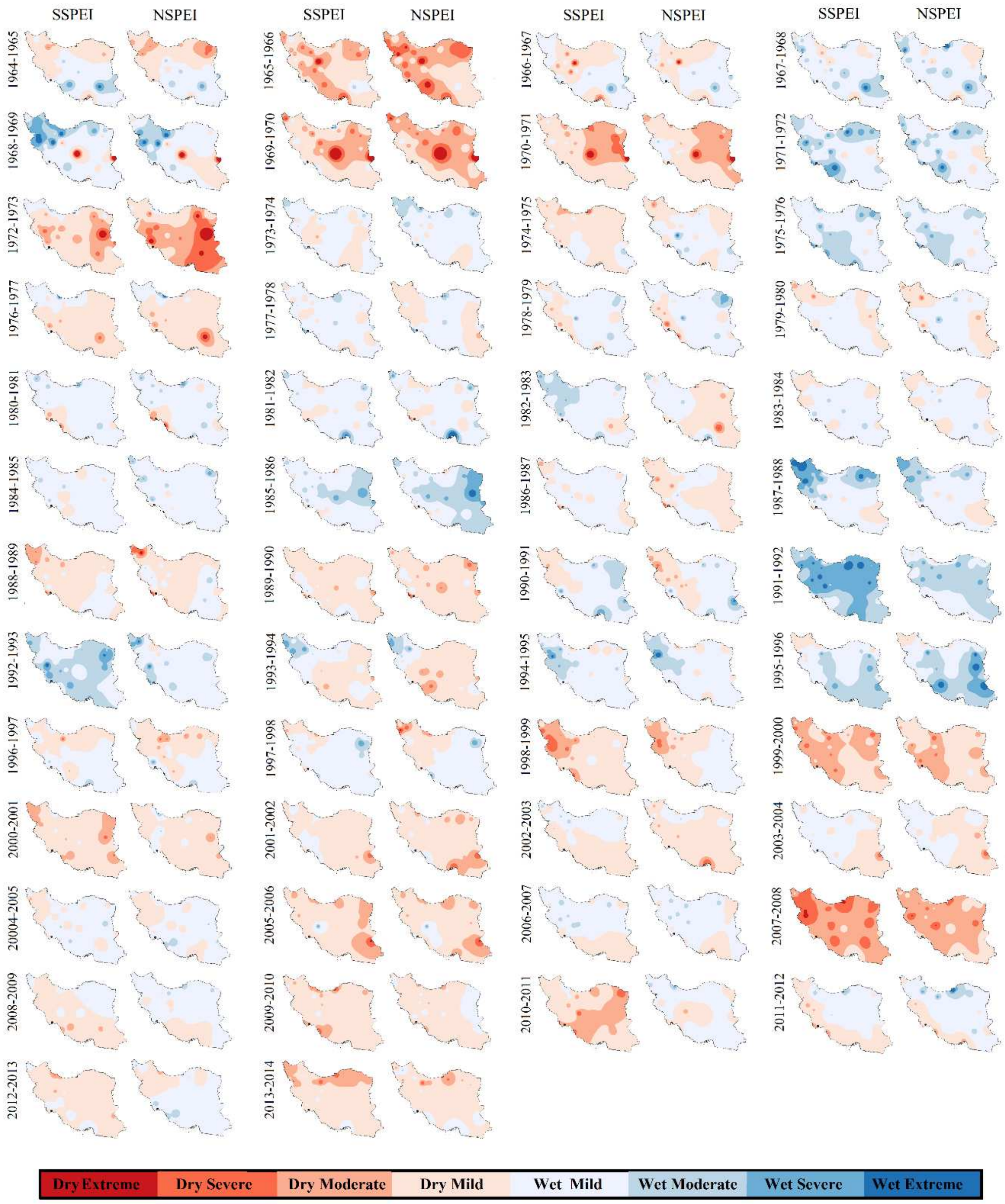

Fig. 11. Spatiotemporal variations of the drought and wet period classes for SSPEI and NSPEI over Iran for the water years (October-September) of 1964/65 - 2013/14.

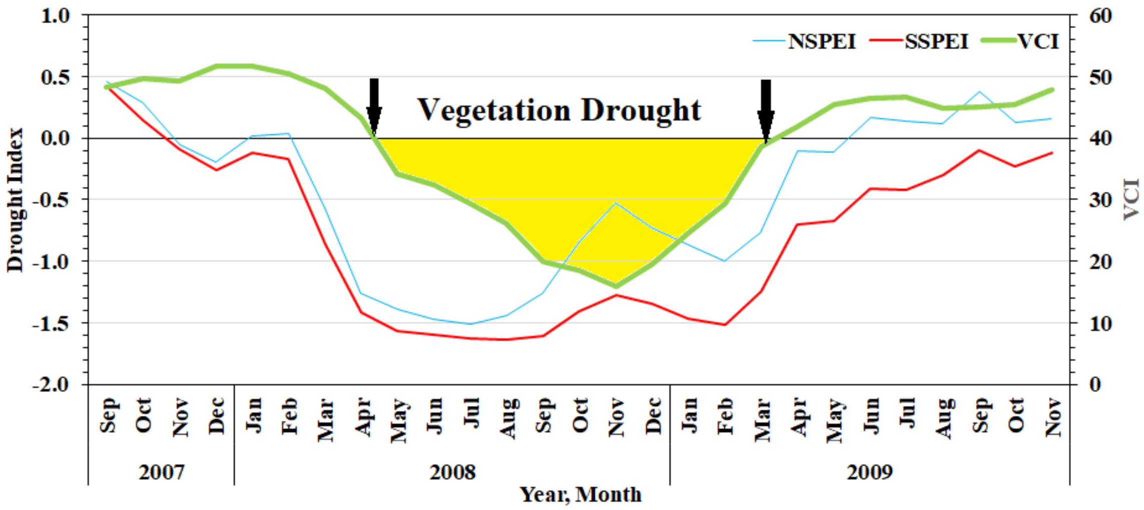

Fig. 12. The average series of SSPEI, NSPEI, and VCI across the studied stations during the September 2007 to November 2009. The reference line is at zero for the left y-axis and at 40 for the right y-axis.